Updates of CTEQ-TEA (Tung et al.) PDF Analysis

C.-P. Yuan
Michigan State University
In collaboration with
CTEQ-TEA

March 14, 2106

PDF4LHC Meeting@
CERN, Switzerland

CTEQ-TEA group

- CTEQ – Tung et al. (TEA)

in memory of Prof. Wu-Ki Tung,

who established CTEQ Collaboration in early 90's

- Current members:

Sayipjamal Dulat (Xinjiang U.),

Tie-Jiun Hou, Pavel Nadolsky (Southern Methodist U.), Jun Gao (Argonne Nat. Lab.), Marco Guzzi (U. of Manchester), Joey Huston, Jon Pumplin, Dan Stump, Carl Schmidt, CPY (Michigan State U.)

Outline

arXiv: 1506.07443

- Brief overview of CT14 global analysis
- Impact of HERA I + II data on CT PDF analysis: **CT14HERA2**
- Replicas of CT14 PDFs: **CT14MC**
- Implications of CMS W^+W^- data to photon PDFs: **CT14QED**
- Conclusion

Overview of CT14 analysis

- CT10 includes only pre-LHC data
- CT14 is the first CT analysis including LHC Run 1 data
- CT14 also includes the new Tevatron D0 Run 2 data on W-electron charge asymmetry
- CT14 uses a more flexible parametrization in the non-perturbative PDFs.
- We have published its results at NNLO, NLO and LO.

Produce 90% C.L. error PDF sets from Hessian method, scaled by 1/1.645 to obtain 68% C.L. eigenvector sets.
For NNLO, Chi^2/d.o.f is about 1.1 for about 3000 data points included in the fits.

Experimental Data for CT14

- Based on CT10 data set, but updated with new HERA F_L and F_2^c , and drop Tevatron Run 1 CDF and D0 inclusive jet
- Included some LHC Run 1 (at 7 TeV) data:

  ATLAS and LHCb W/Z production,
  ATLAS, CMS and LHCb W-lepton charge asymmetry,
  ATLAS and CMS inclusive jet
- Replace old by new D0 (9.7 1/fb) W-electron rapidity asymmetry data

Theory Analysis in CT14

- CT14 has 26 shape parameters, plus four extreme sets for describing s- and g-PDFs in small-x region. In comparison, CT10 has 24 shape parameters, plus two extreme sets for describing g-PDFs in small-x region.
- More flexible parametrization – gluon, d/u at large x, and both d/u and dbar/ubar at small x, strangeness (assuming sbar = s)
- Non-perturbative parametrization form:

$$x\, f_a(x) = x^{a_1}\,(1-x)^{a_2}\, P_a(x)$$

where $P_a(x)$ is expressed as a linear combination of Bernstein polynomials to reduce the correlation among its coefficients.

Theory Analysis in CT14

- Choose experimental data with $Q^2 > 4\ GeV^2$ and $W^2 > 12.5\ GeV^2$ to minimize high-twist, nuclear correction, etc., and focus on perturbative QCD predictions.
- PDFs are parametrized at Q=1.3 GeV.
- Take $\alpha_s(Mz) = 0.118$, but also provide α_s-series PDFs.
- Use s-ACOT-χ prescription for heavy quark partons, and take pole mass M_c =1.3 GeV and M_b=4.75 GeV
- NNLO calculations for DIS, DY, W, Z, except jet (at NLO).
- Correlated systematic errors are taken into account.
- Check Hessian method results by Lagrangian Multiplier method which does not assume quadratic approximation in chi-square.

Impact of HERA I + II data on CT PDF analysis:

CT14HERA2

PDF parametrization in CT14HERA2

We used the CT14 PDF functional forms at initial scale Q_0.

$$x\, f_a(x, Q_0) = x^{a_1}\,(1-x)^{a_2}\,P_a(x)$$

- CT14HERA2 has 29 shape parameters, plus two extreme sets for describing g-PDF in small-x region. In comparison, CT14 has 26 shape parameters, plus four extreme sets for describing s- and g-PDFs in small-x region.

- To relax the dv/uv and dbar/ubar ratios as x -> 1, and to add one more shape parameters (in total 3) for describing s-PDF.

HERAI +II data

- H1 and ZEUS experiments at HERA for neutral current and charged current e+p, e-p scattering collected ~1/fb of data.
- Ep =920, 820, 575 and 460 GeV and Ee=27.5 GeV.

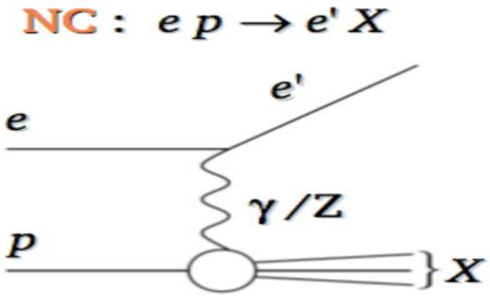

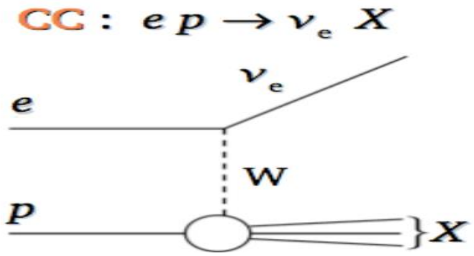

arXiv:1506.06042

Cross sections for NC interactions have been published for

$0.045 < Q^2 < 50000\ \mathrm{GeV}^2 \qquad 6.\,10^{-7} < x_{Bj} < 0.65$

Cross sections for CC interactions have been published for

$$200 \leq Q^2 \leq 50000\,\mathrm{GeV}^2 \text{ and } 1.3 \cdot 10^{-2} \leq x_{\mathrm{Bj}} \leq 0.40$$

- HERAI+II data has 1119 data points with

  $Q^2 > 4\ GeV^2$ and $W^2 > 12.5\ GeV^2$,

  162 correlated systematic errors,

  7 procedural uncertainties;

  separated into four sets, depending on whether e+ or e- beam, neutral or charged current, at various collider energies.
- HERA-1 data has 579 data points with

  $Q^2 > 4\ GeV^2$ and $W^2 > 12.5\ GeV^2$,

  110 correlated systematic errors,

  4 procedural uncertainties.
- CT14 with HERA1 has about 3000 data points.
- After replacing the HERA I with HERA I+II data, there are about 3300 data points in total ,in which we have removed NMC muon-proton data (ID=106, with 201 data points). Its chi^2/npt is about 1.85 in CT14 fit.

Impact of the HERAI +II data on the fit

Summary of the chi2 values for the HERA run I and HERA1+2 measurements in both CT14 and CT14HERA1+2 fits

	$\chi^2_{\text{HERA I}}$; $N_{pts} = 549$	$\chi^2_{\text{HERA1+2}}$; $N_{pts} = 1119$
CT14NLO	590	1360
CT14NNLO	591	1429
CT14HERA1+2(NLO)	576	1326
CT14HERA1+2((NNLO)	582	1358

The distribution of the χ^2-residuals of HERA I and HERA2 ensembles in the (x, Q) plane for the CT14Hera2 fit.

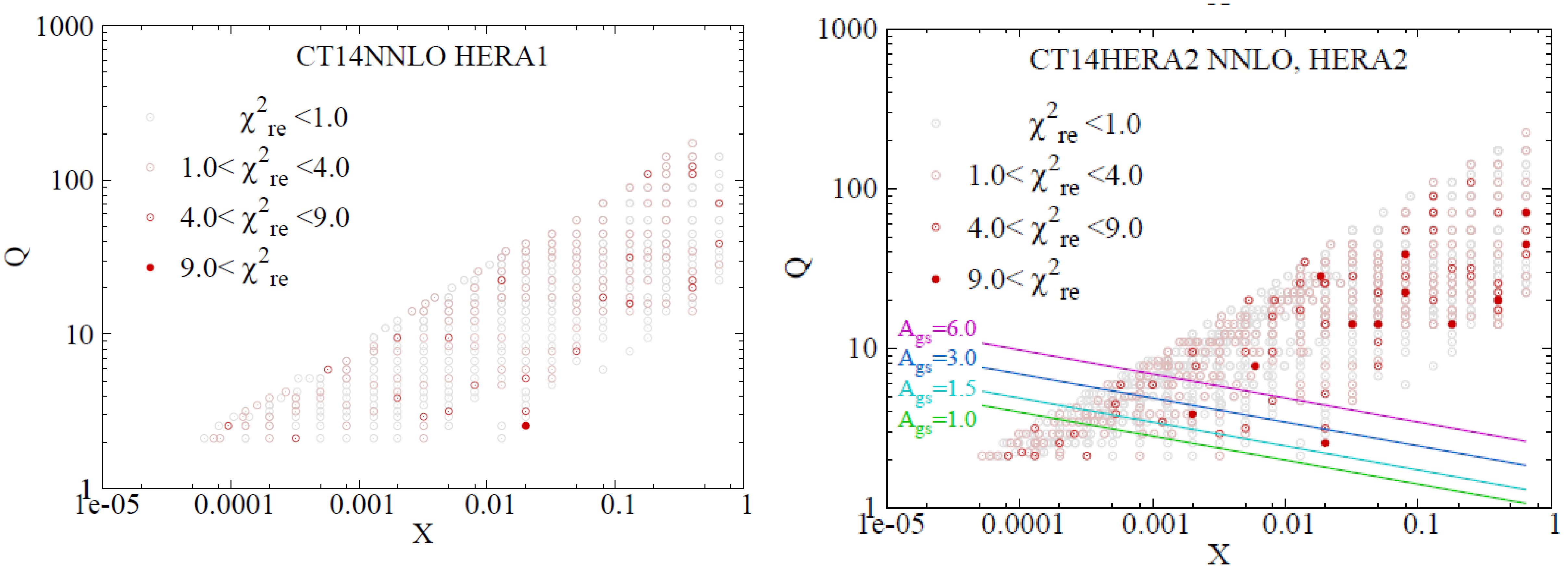

HERA I

NNLO fits

HERA I+II

The distribution of the χ^2-residuals of HERA I and HERA2 ensembles in the (x, Q) plane for the CT14Hera2 fit

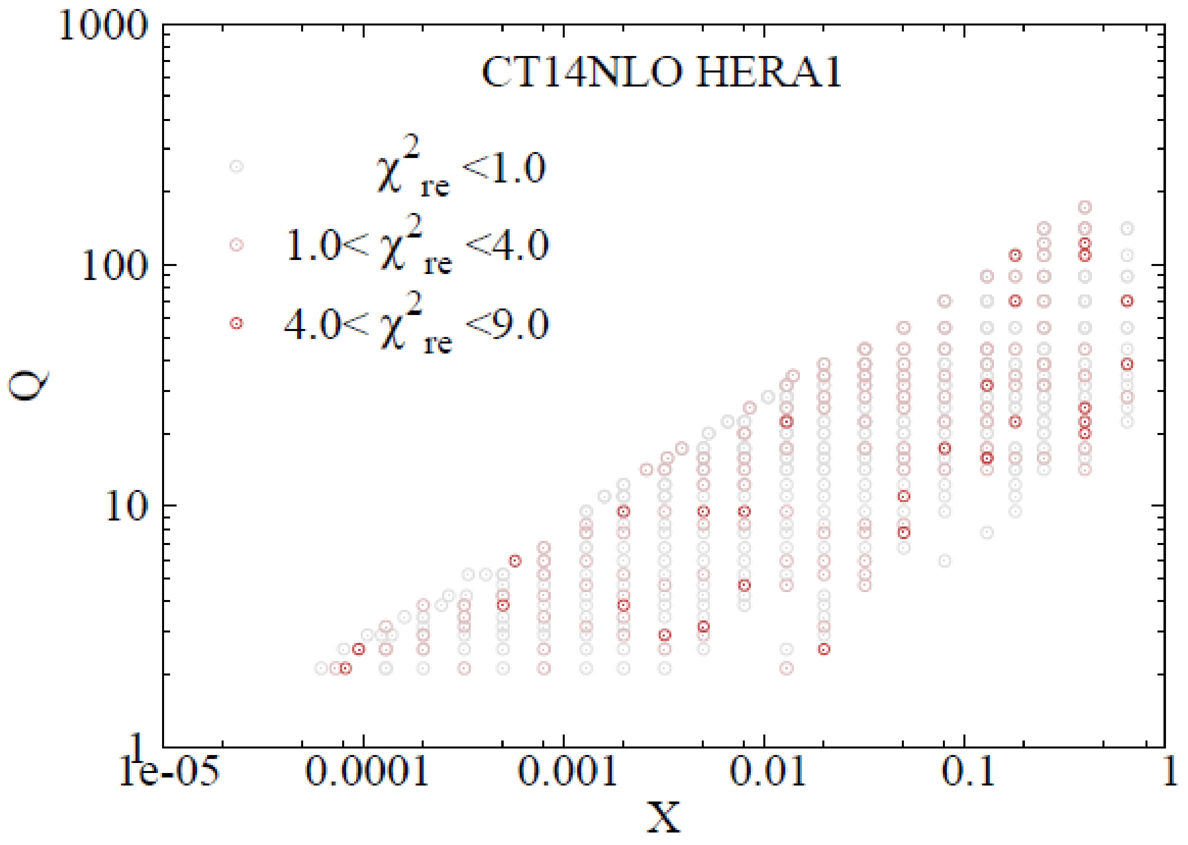

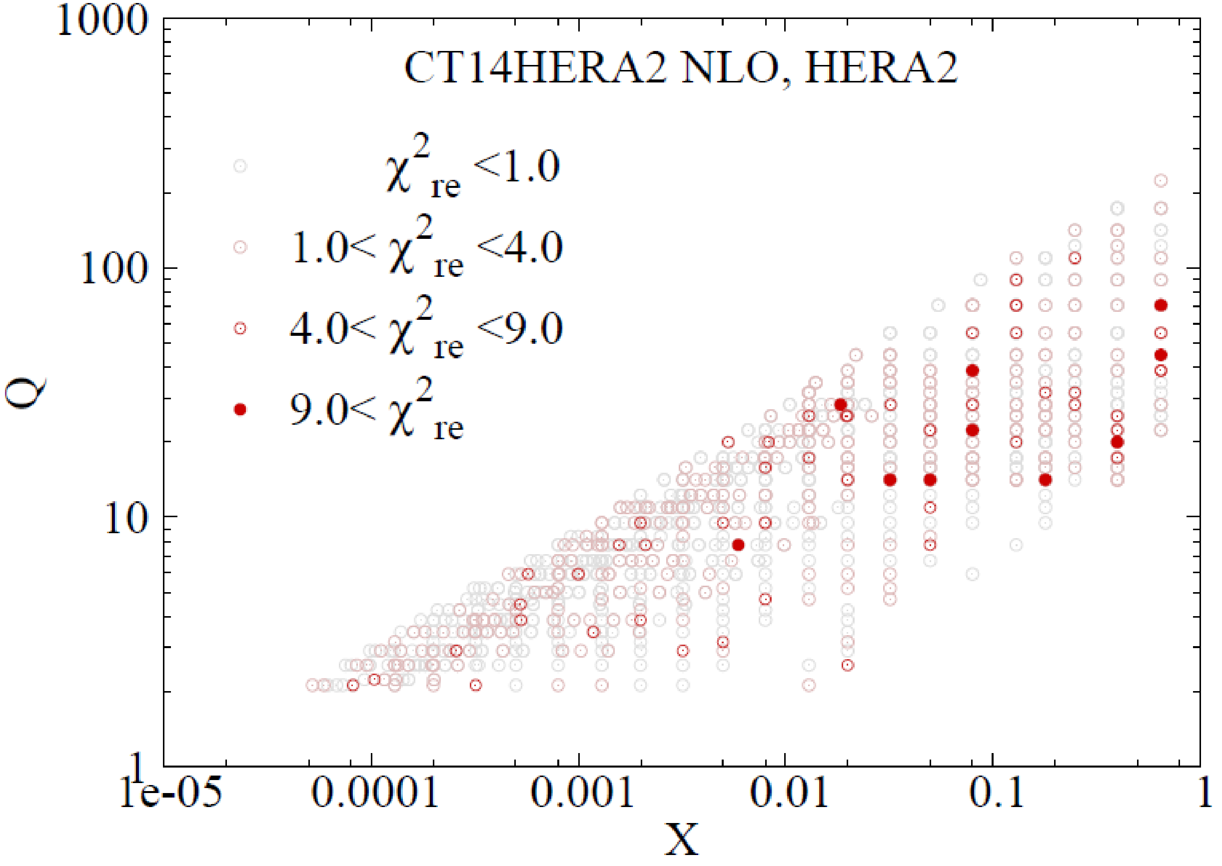

HERA I

NLO fits

HERA I+II

NNLO vs. NLO fits

1.21 for NNLO fit

1.19 for NLO fit

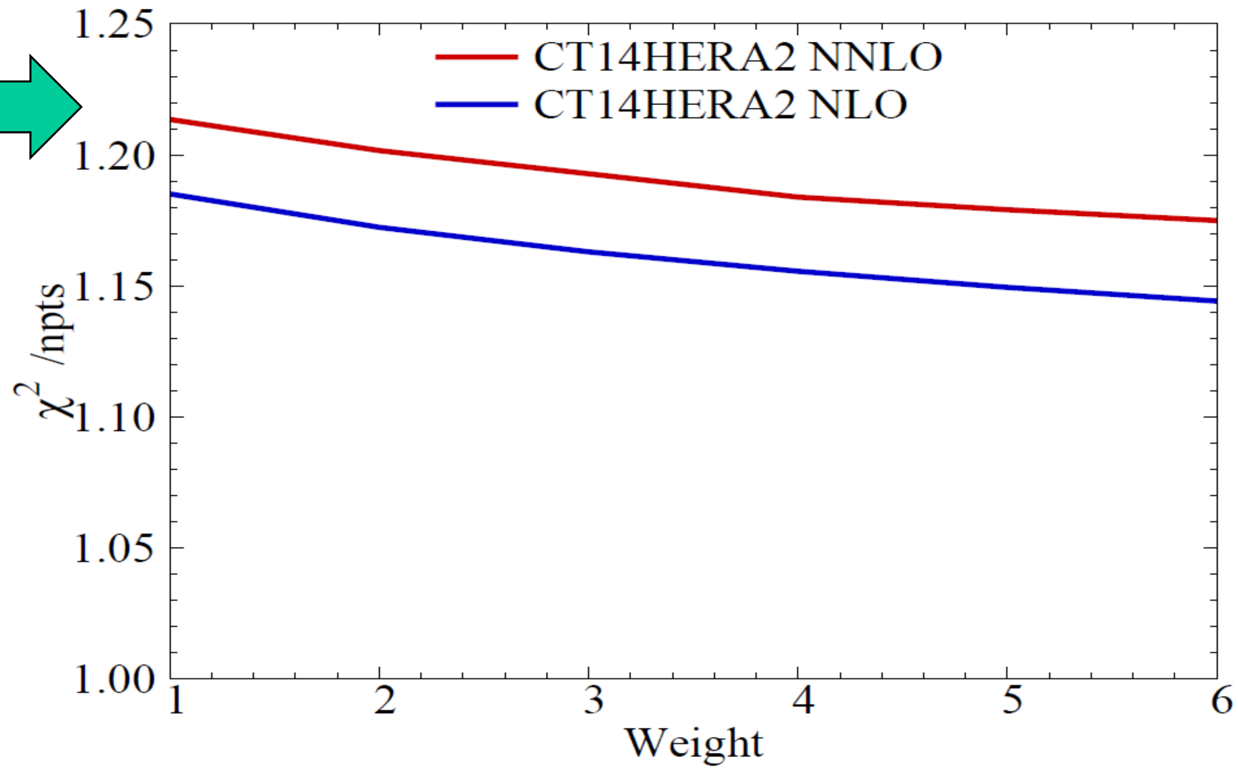

Dependence of χ^2/d.o.f on various weights assigned to HERA2 data ensemble.

Replace HERA I combined data by the new HERA 1+2 combined data in the CT14HERA2 analysis. If we increase the weight of the of HERA 1+2 combined data in the global fit, its chi2/Npt decreases, as it should be, because it can fit better. However, when the weight of this data is too large, the chi2/Npt of BCDMS F2 muon-deuteron data and CMS jet data increase by noticeable amount.

Correlation angle (g-PDF vs. CMS jet data)

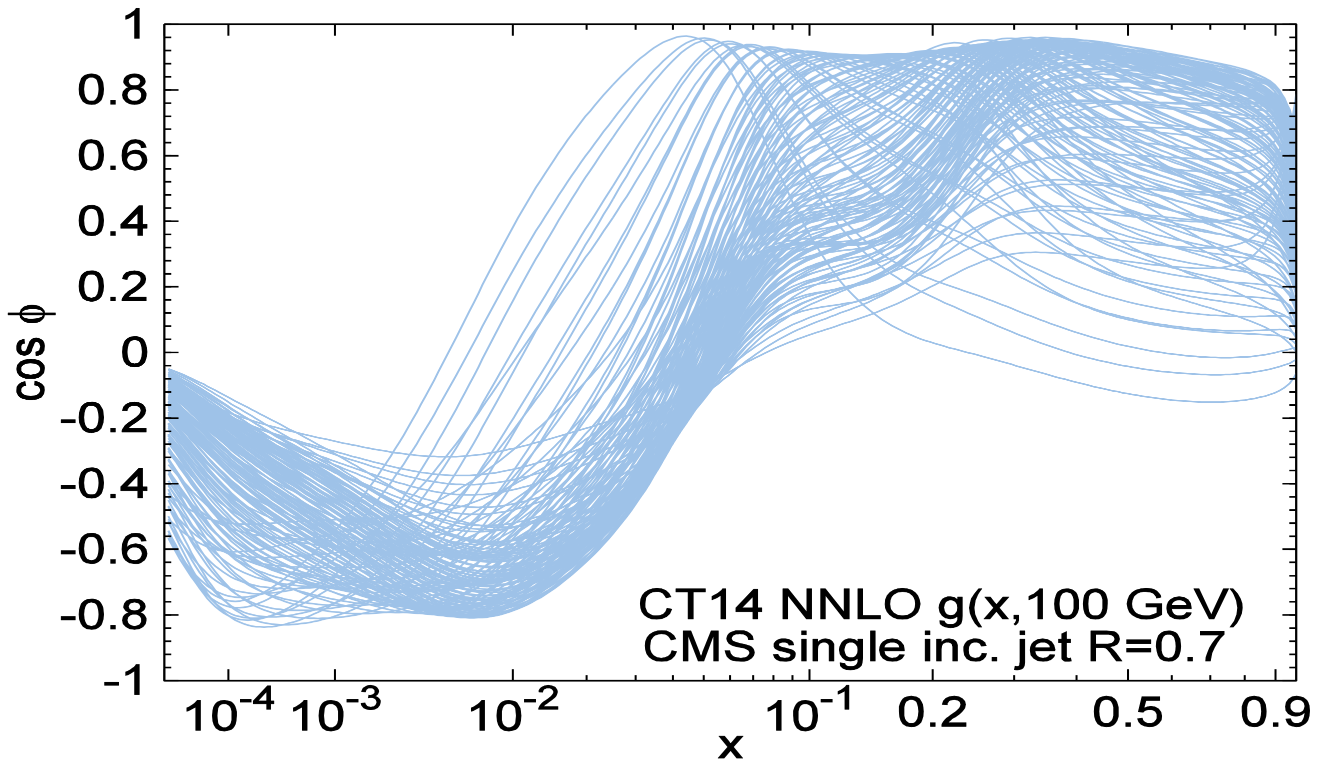

- Jet data is highly correlated to g-PDF at large x region and anti-correlated in small-x region.
- Precision HERA data are sensitive to g-PDF in small-x region, hence, correlated to CMS jet data.

CT14HERA2 vs. CT14
g and u PDFs

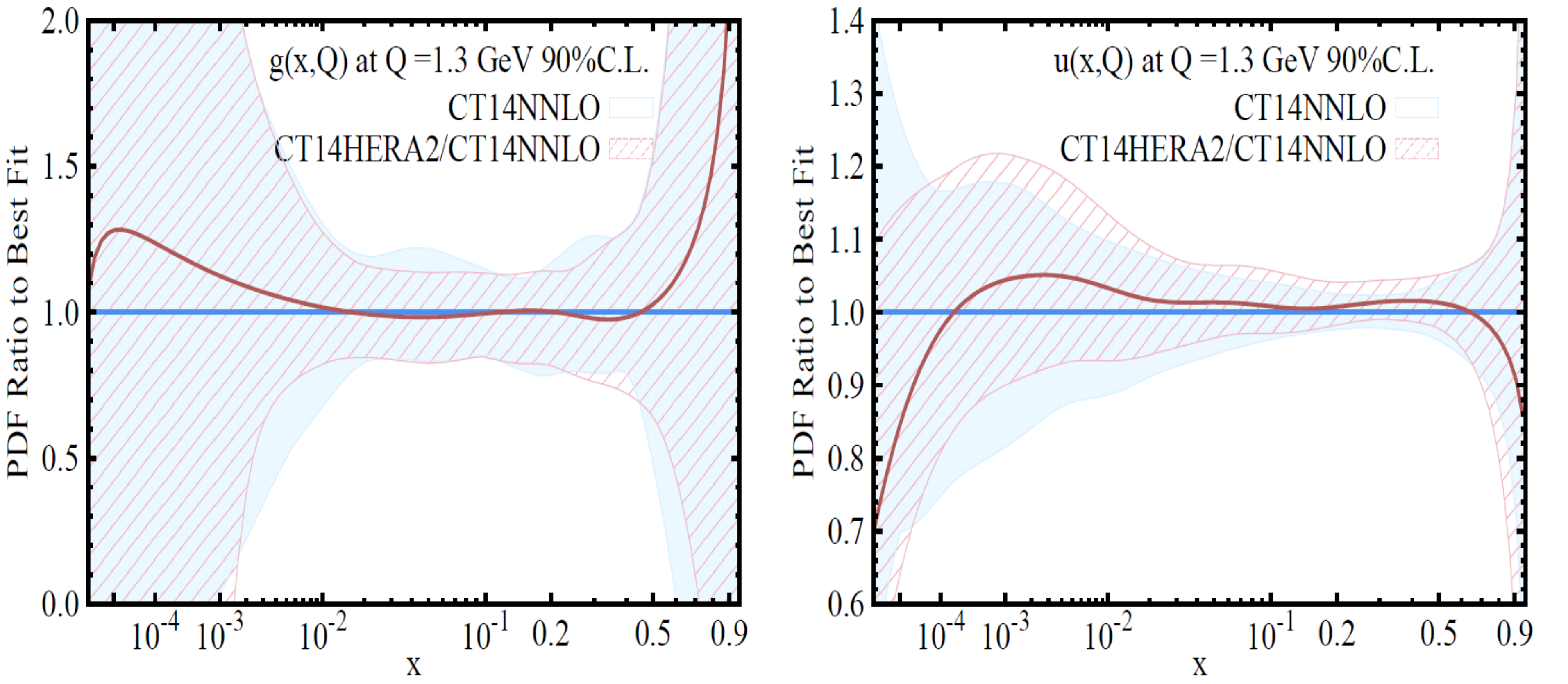

Comparison of 90% C.L. uncertainties on g and u PDFs for the CT14 NNLO (solid blue) and CT14H2 NNLO (red hatched) error ensembles. Both error bands are normalized to the respective central CT14 NNLO PDFs.

d and s PDFs

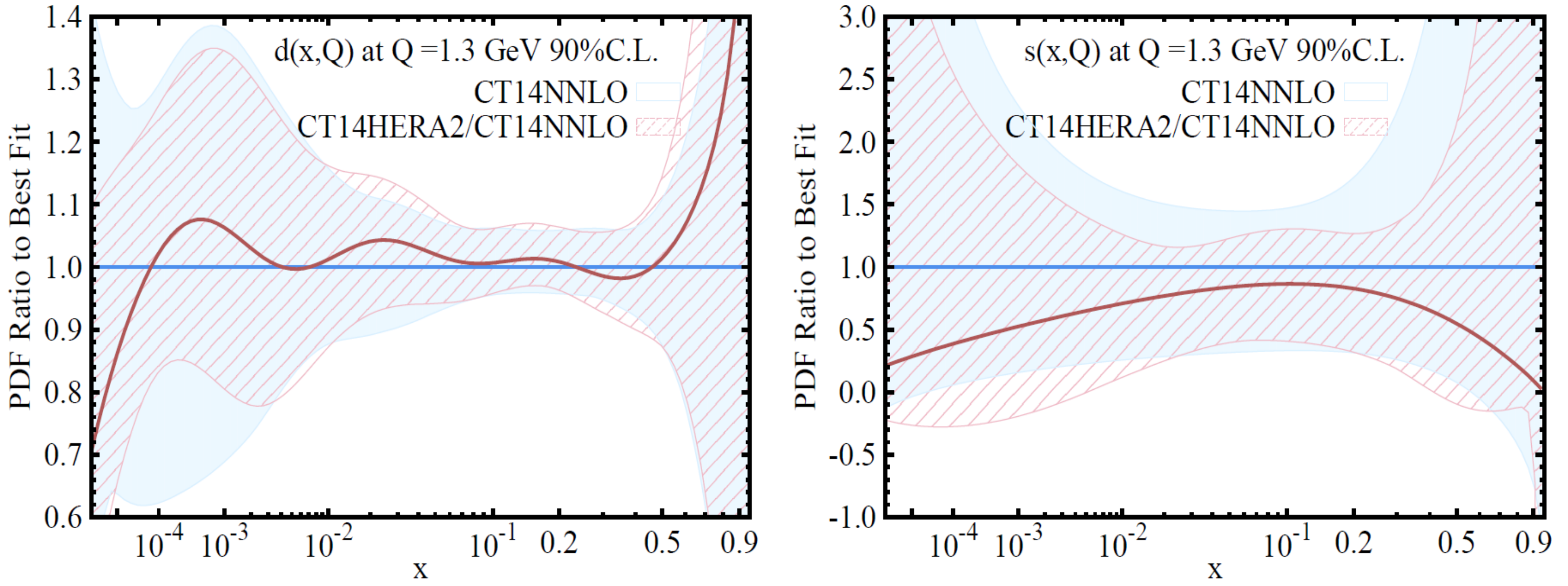

Comparison of 90% C.L. uncertainties on d and s PDFs for the CT14 NNLO (solid blue) and CT14H2 NNLO (red hatched) error ensembles. Both error bands are normalized to the respective central CT14 NNLO PDFs.

Ubar and dbar PDFs

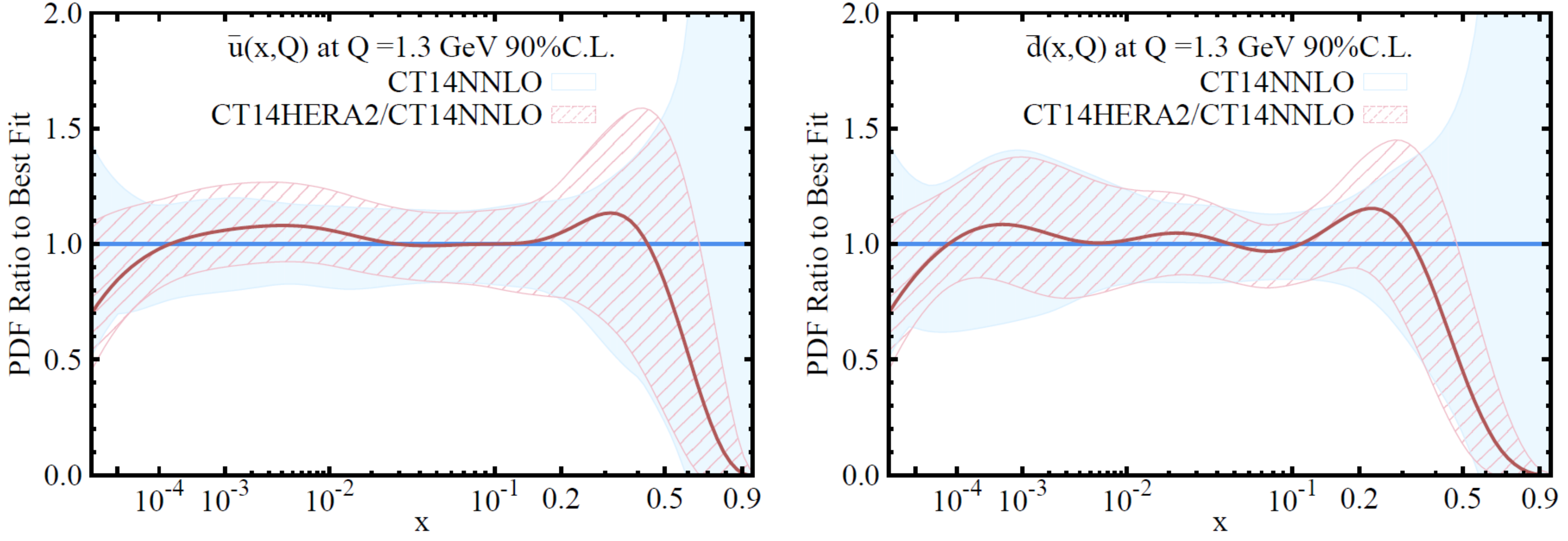

Comparison of 90% C.L. uncertainties on ubar and dbar PDFs for the CT14 NNLO (solid blue) and CT14H2 NNLO (red hatched) error ensembles. Both error bands are normalized to the respective central CT14 NNLO PDFs.

d/u and dbar/ubar PDFs

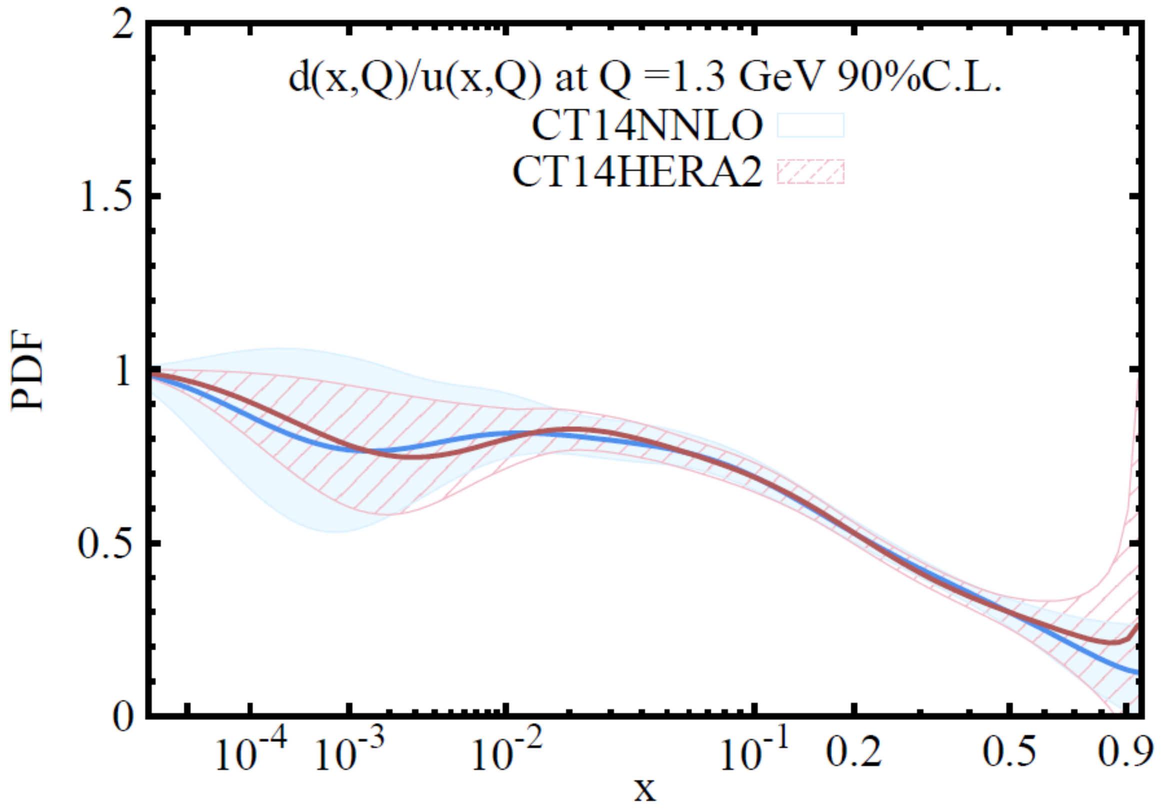

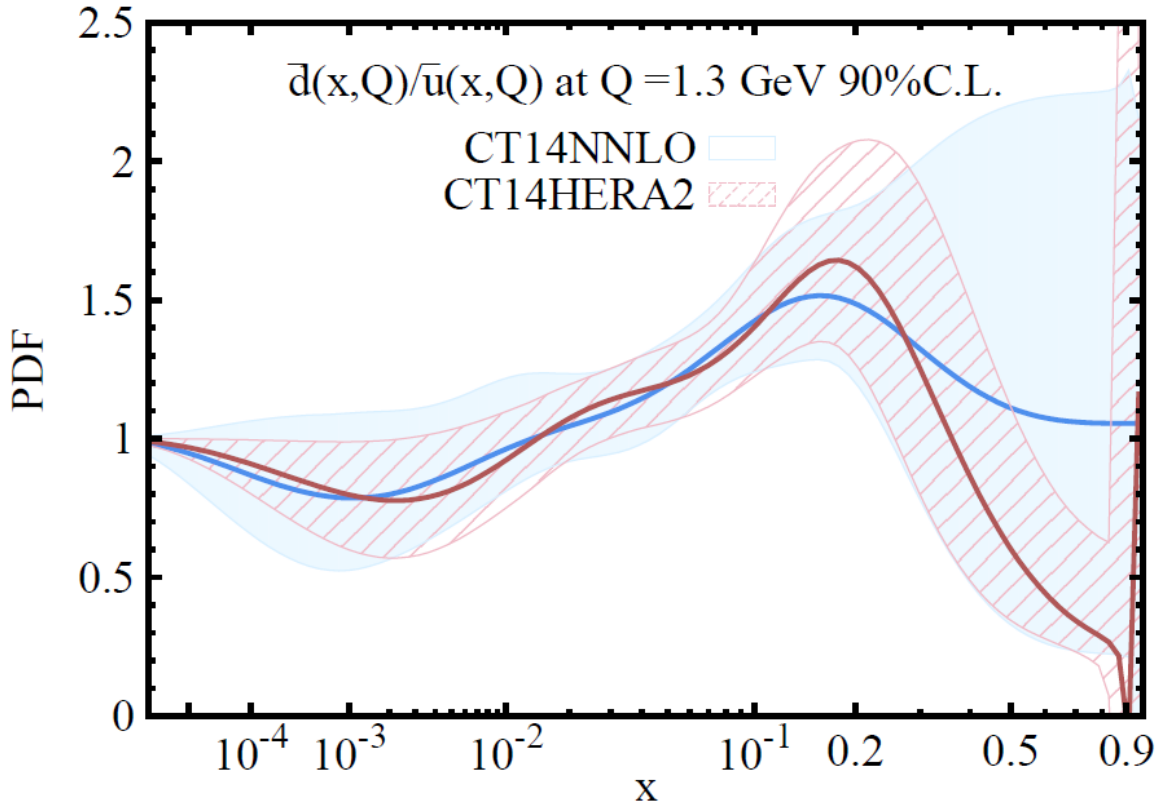

Comparison of 90% C.L. uncertainties on d/u and dbar/ubar PDFs for the CT14 NNLO (solid blue) and CT14H2 NNLO (red hatched) error ensembles. Both error bands are normalized to the respective central CT14 NNLO PDFs.

(s+sbar)/(ubar+dbar) PDFs

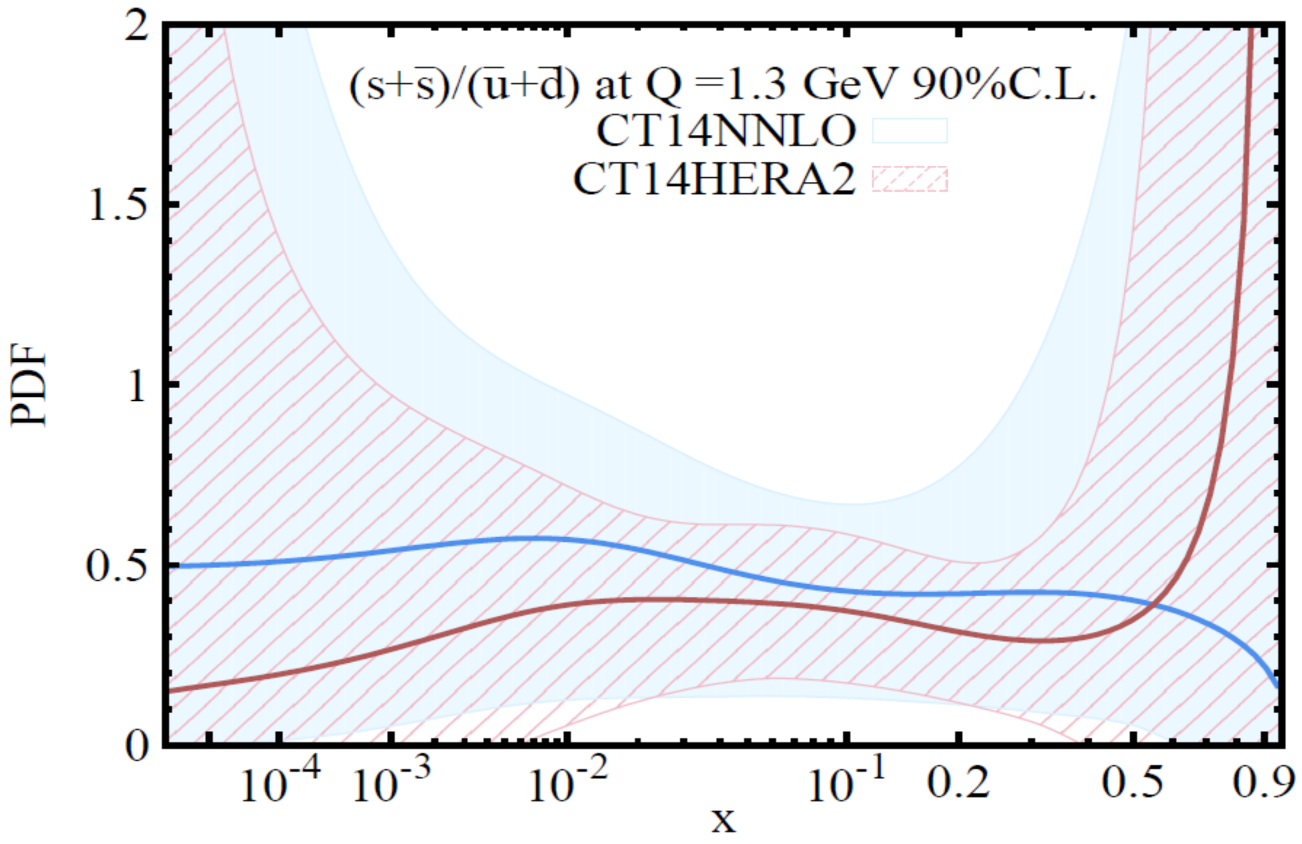

Comparison of 90% C.L. uncertainties on (s+sbar)/(ubar+dbar) PDFs for the CT14 NNLO (solid blue) and CT14H2 NNLO (red hatched) error ensembles. Both error bands are normalized to the respective central CT14 NNLO PDFs.

Impact of Q Cut on fits

1.21 for
NNLO fit

1.19 for
NLO fit

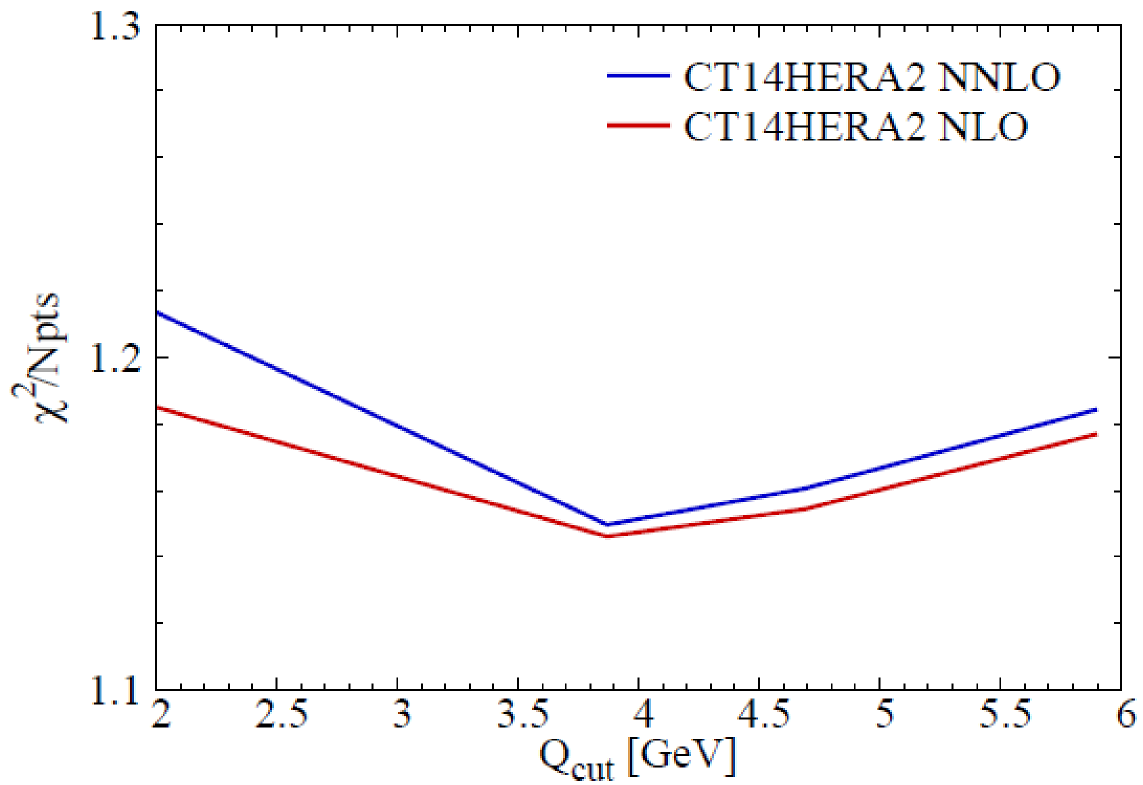

- Our nominal Q cut is 2 GeV.
- Chi2/Npt of CT14HERA2 NLO fit is somewhat smaller than NNLO fit for Q cut less than 4 GeV.

Different cuts on x-Q plane

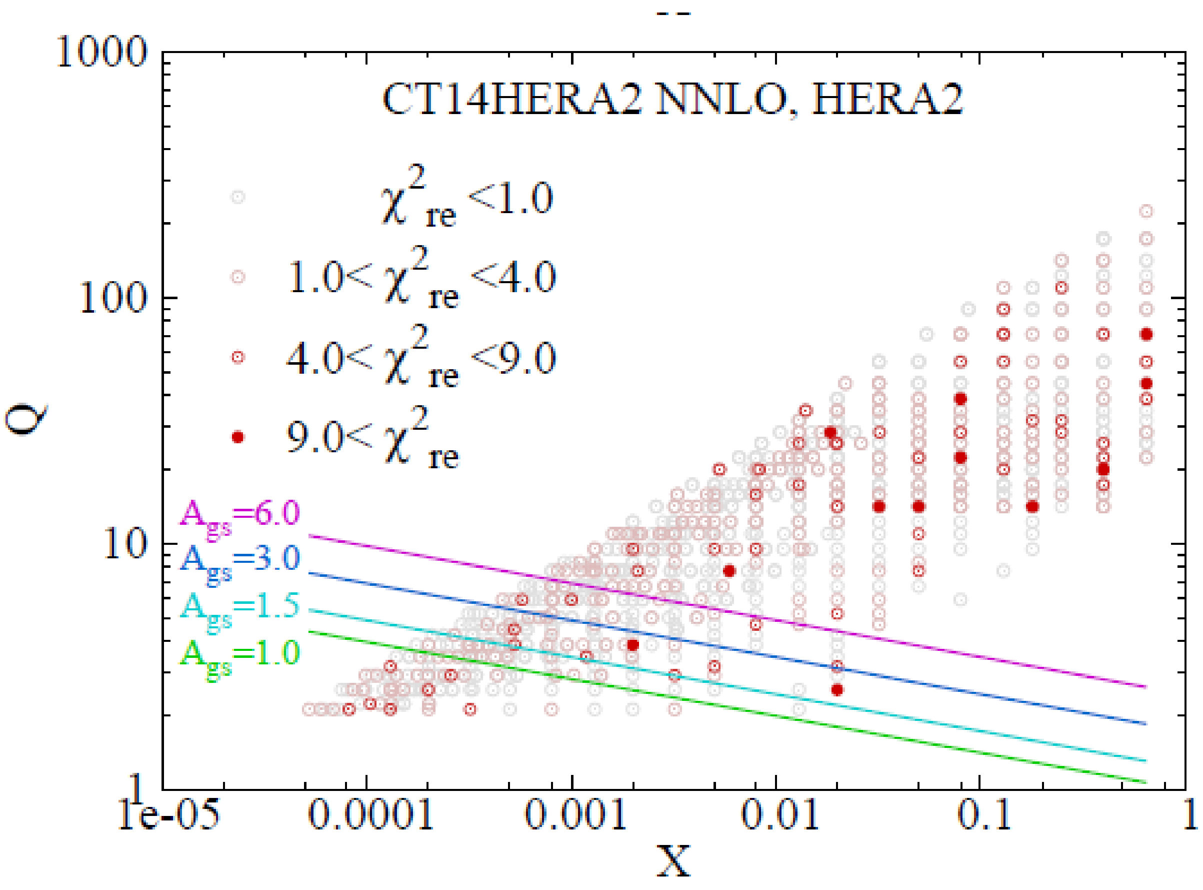

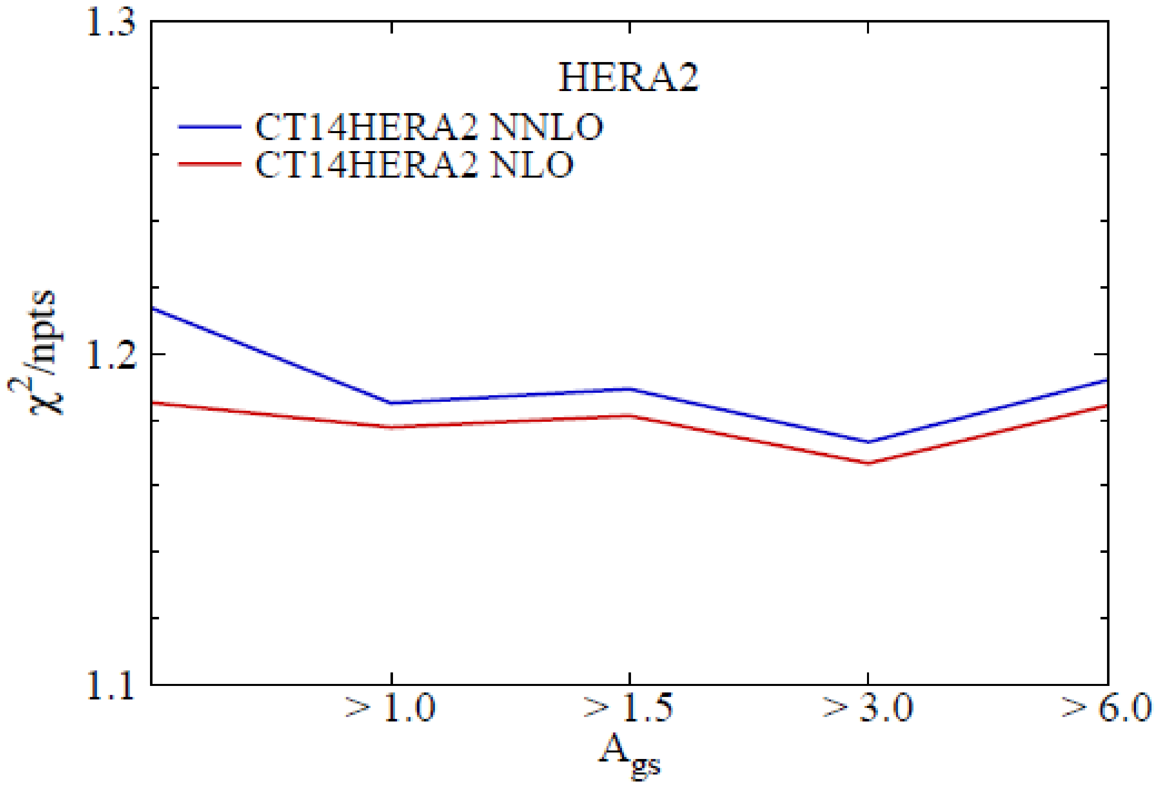

$$A_{gs} = Q^2 x^{0.3}$$

The ratios of W^+ to W^- and $(W^+ + W^-)$ to Z cross sections

- Measured by the ATLAS and CMS collaboration and proved to be powerful tools to constrain PDFs
- The ratio of **W^+ to W^-** boson cross section is mostly sensitive to the difference of u valence and d valence quark distributions.
- **While the ratio of $(W^+ + W^-)$ to Z boson cross section constrains the strange-quark distribution.**

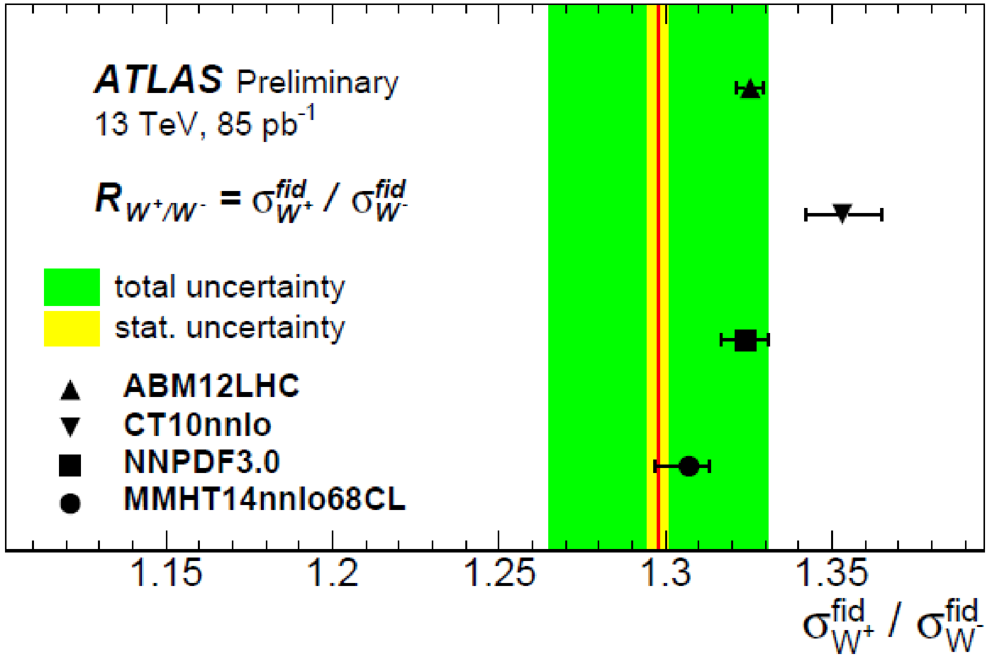

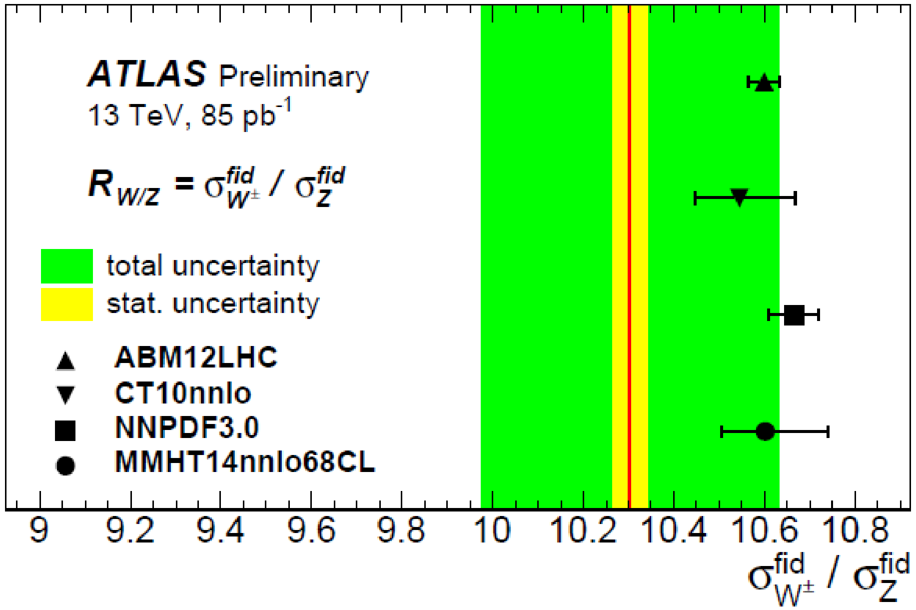

The ratios of W^+ to W^- and (W^++W^-) to Z cross sections
CT14HERA2 vs. CT14

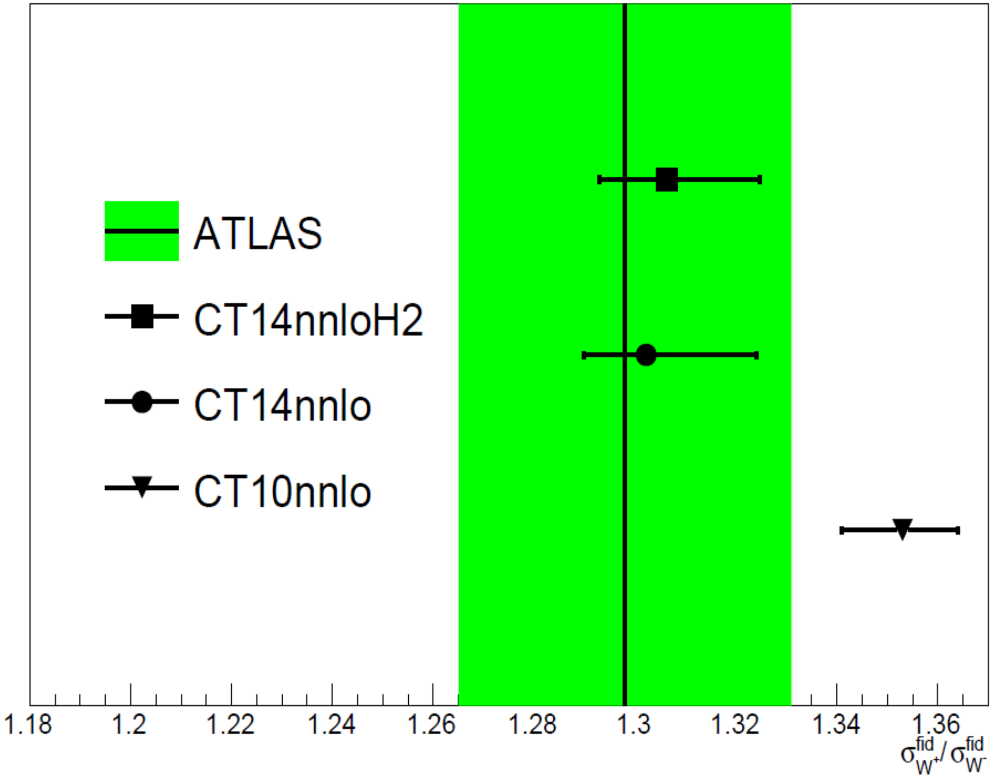

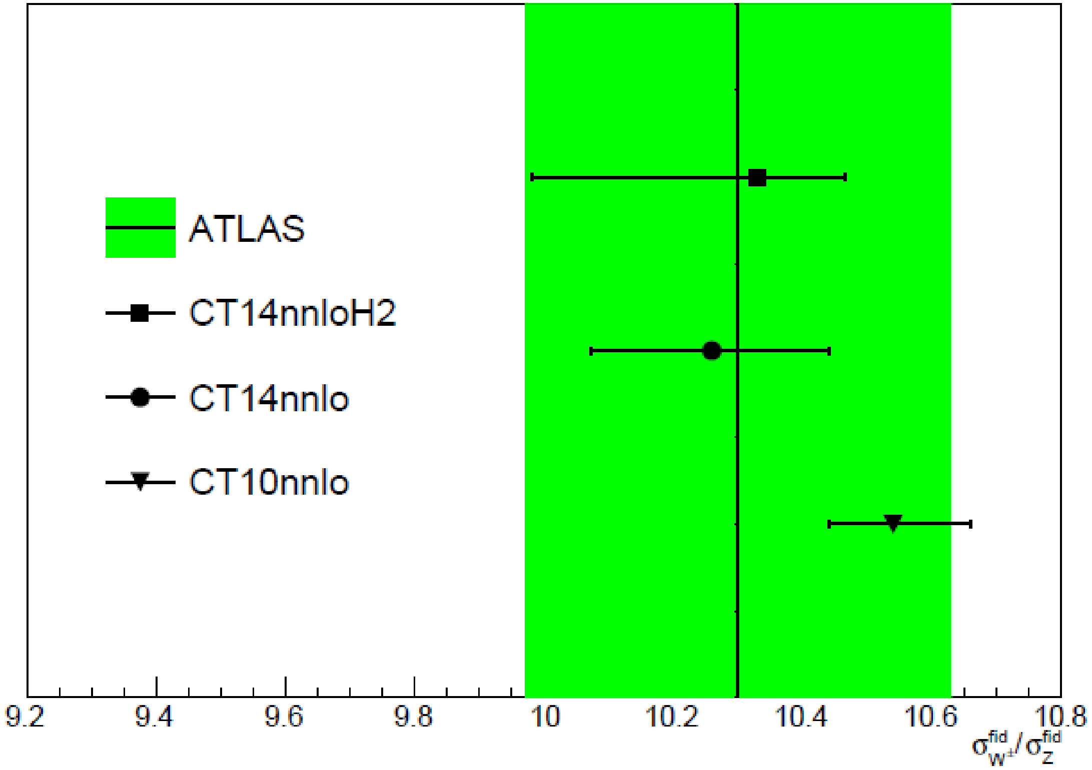

$p_T^l > 25\ GeV\ , \quad |\eta_l| < 2.5\ , \quad 66 < m_{ll} < 116\ GeV$

$p_T^l > 25\ GeV\ , \quad p_T^\nu > 25\ GeV\ , \quad |\eta_l| < 2.5\ , \quad m_T > 50\ GeV$

Replicas of CT14 PDFs

CT14MC

Monte-Carlo replicas for CT14 asymmetric errors

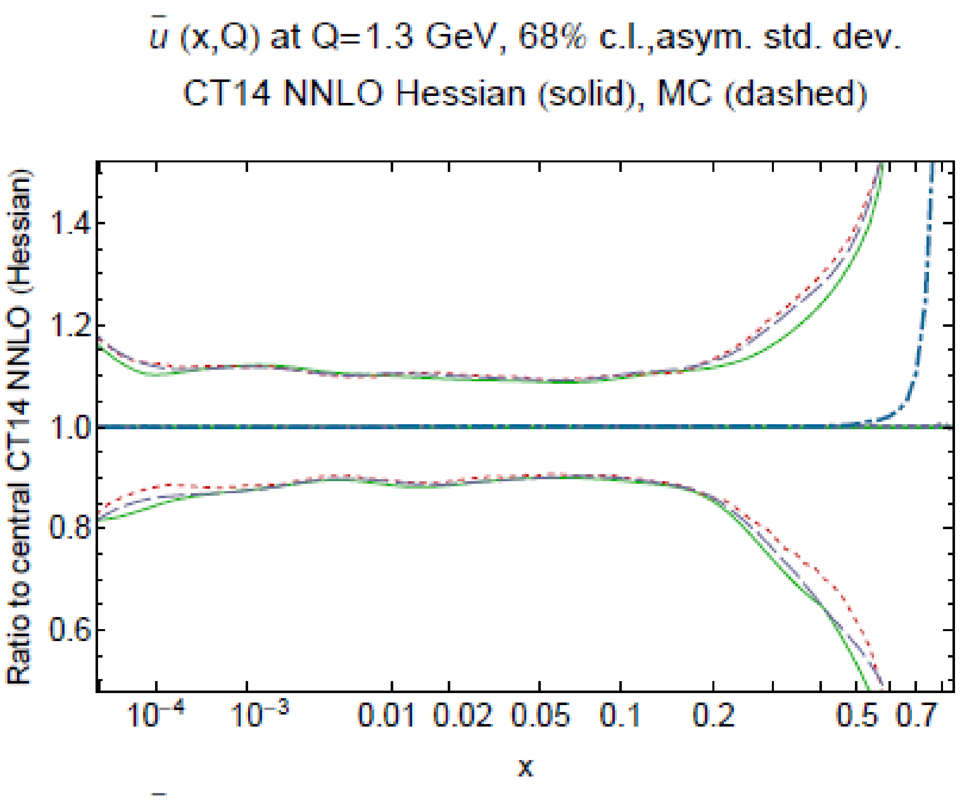

Green: Hessian 68% c.l. errors
Blue: Asymmetric MC replicas

Generation of MC replicas from CT14 Hessian eigenvector sets

MC replicas for PDFs $f_a(x,Q) \equiv f \ldots$

- are constructed from the best-fit (central) PDF values f_0 and 68% c.l. extreme displacements $f_{\pm i}$ along eigenvector directions $\vec{\mathrm{u}}_i, i = 1, \ldots, 28$ in parameter space near χ^2 minimum
- retain exact information about boundaries of 68%/90% probability regions; approximate probability everywhere using Gaussian approximation

- approximate asymmetric Hessian errors using modified standard deviations

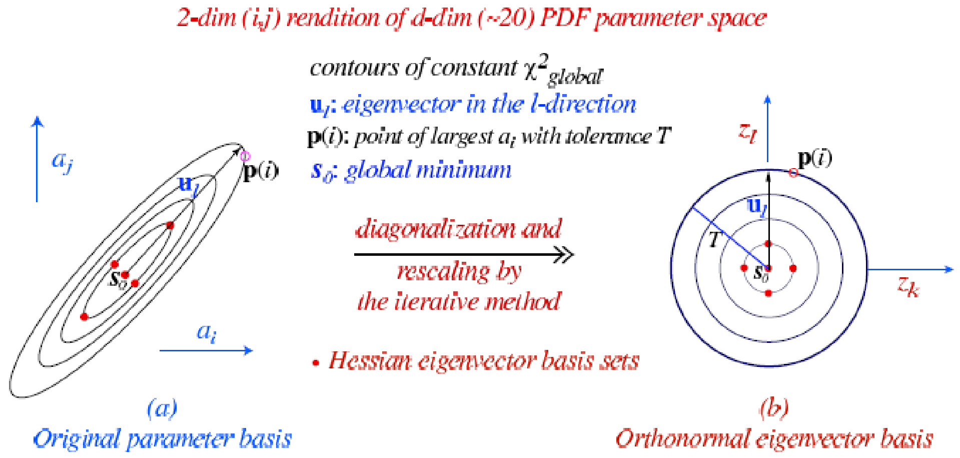

Sources of asymmetry of PDF errors for QCD predictions

C T E Q

$$\chi^2 \Rightarrow \text{PDFs } f_a(x,Q) \Rightarrow \text{ Cross sections } X$$

1. The asymmetry of χ^2 is usually mild near the minimum; can approximate

$$\chi^2 \approx \chi_0^2 + \sum_{i=1}^{D} R_i^2 \ ,$$

where R_i (rescaled z_i) obeys the standard normal distribution:

$$Probability(\{R\}) \sim e^{-\sum_{i=1}^{D} R_i^2/2}$$

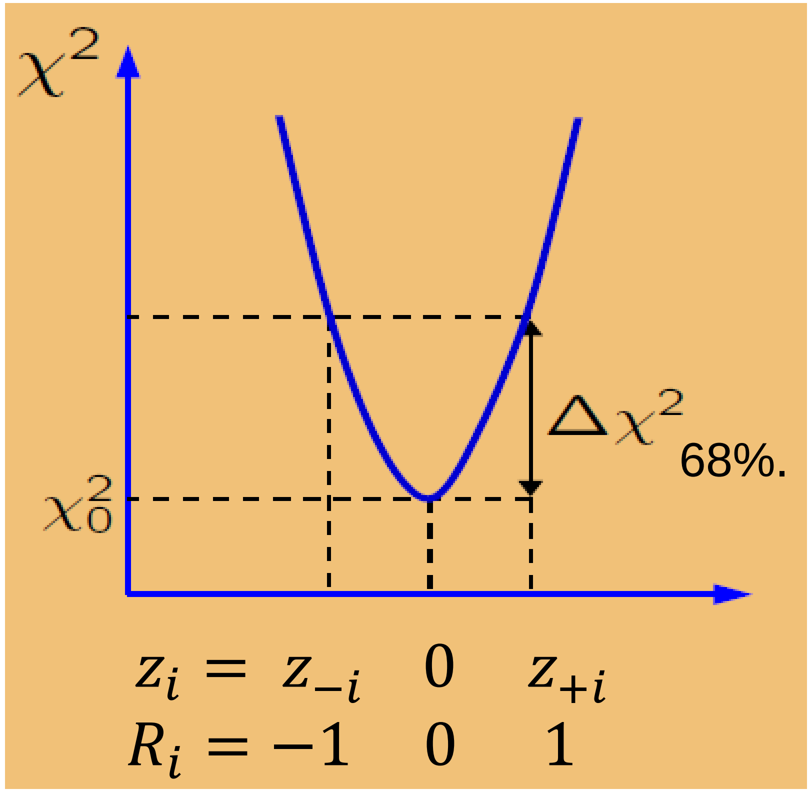

$$f_{\pm i}(\{R\}) = f(0,0,\dots,R_i = \pm 1,\dots,0)$$

$$f_{\pm i,\pm j}(\{R\}) = f\left(0,\dots,R_i = \pm 1,\dots,R_j = \pm 1,\dots,0\right)$$

Sources of asymmetry of PDF errors for QCD predictions

$\chi^2 \Rightarrow$ PDFs $f_a(x,Q) \Rightarrow$ Cross sections X

2. PDFs and cross sections are generally asymmetric functions of R_i

$$X(\{R\}) = X(\{0\}) + \sum_{i=1}^{D} \frac{\partial X}{\partial R_i} R_i + \frac{1}{2} \sum_{i,j=1}^{D} \frac{\partial^2 X}{\partial R_i \partial R_j} R_i R_j + \cdots$$

Evaluate partial derivatives by finite differences

$$\frac{\partial X}{\partial R_i} \approx \frac{X_{+i} - X_{-i}}{2}$$

need $2D$ eigenvector sets

$$\frac{\partial^2 X}{\partial R_i^2} \approx X_{+i} + X_{-i} - 2X_0$$

need $2D$ eigenvector sets

$$\frac{\partial^2 X}{\partial R_i \ \partial R_j} \approx \frac{X_{+i,+j} + X_{-i,-j} - X_{+i,-j} - X_{-i,+j}}{4}$$

need $2D(D-1)$ NEW eigenvector sets

Symmetric PDF errors

Keep only linear terms

$$X(\{R\}) = X(\{0\}) + \sum_{i=1}^{D} \frac{X_{+i} - X_{-i}}{2} R_i$$

1. The Hessian method produces a symmetric master formula (Stump, Pumplin, Tung, et al., 1999):

$$\delta_{68}^{H}\ X = |\nabla X| = \frac{1}{2}\sqrt{\sum_i (X_{+i} - X_{-i})^2}$$

2. The MC generation produces N_{rep} symmetric replicas

$$X^{(k)} = X(\{0\}) + \sum_{i=1}^{D} \frac{X_{+i} - X_{-i}}{2} R_i^{(k)}, \qquad k = 1, \ldots, N_{rep}$$

$R_i^{(k)}$ are normally distributed. We choose $N_{rep} = 1000$.

Hessian and MC symmetric errors for PDFs $(X = f)$ ...

… agree well
The MC mean can deviate when the PDFs vanish

The MC error is estimated by the standard deviation of X,

$$\delta_{68}^{MC} X = \sqrt{\langle (X - \langle X \rangle)^2 \rangle}$$

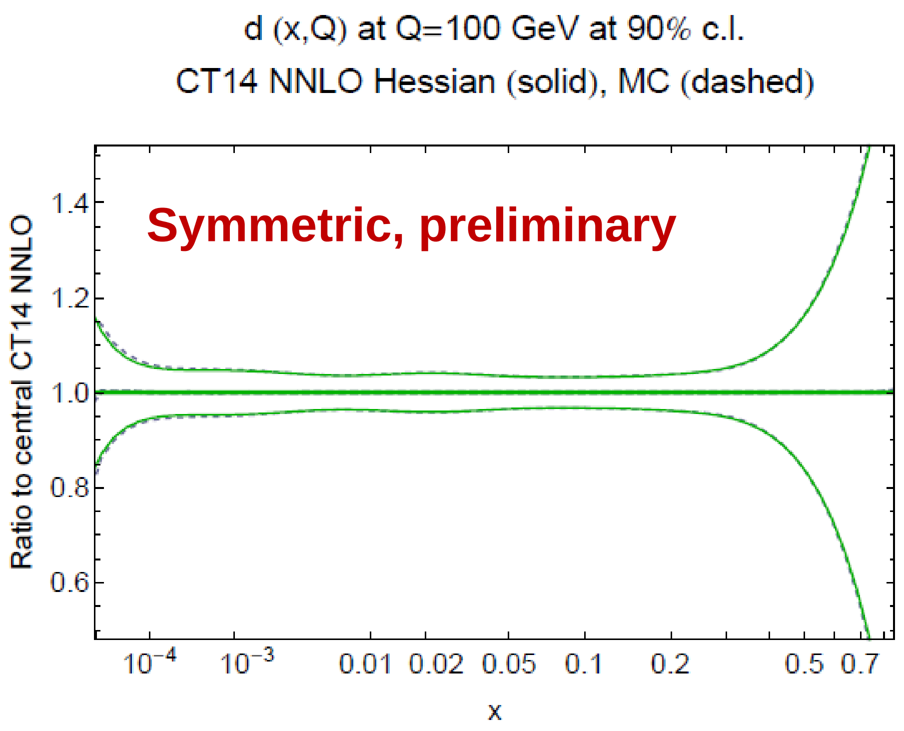

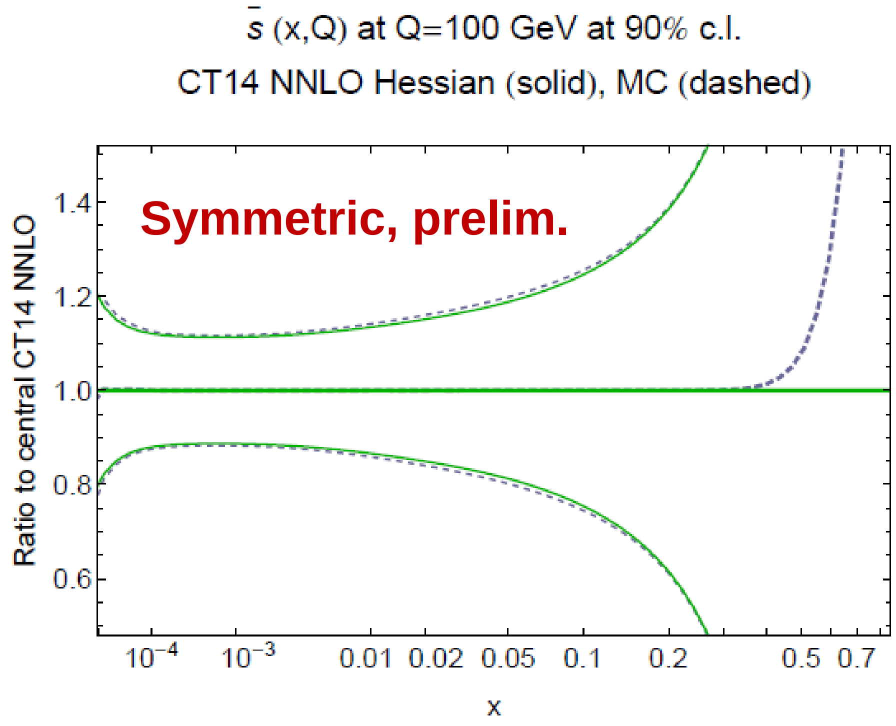

CT14 asymmetric PDF errors

C T E Q

Include the diagonal second derivatives

$$X(\{R\}) = X(\{0\}) + \sum_{i=1}^{D} \frac{X_{+i} - X_{-i}}{2} R_i + \frac{1}{2} \sum_{i,j=1}^{D} (X_{+i} + X_{-i} - 2X_0) R_i^2$$

1. The Hessian method produces asymmetric master formulas (Nadolsky, Sullivan, 2001)

$$\delta_{68}^{H,>} X = \sqrt{\sum_i (max[X_{+i} - X_0, X_{-i} - X_0, 0])^2}$$

$$\delta_{68}^{H,<} X = \sqrt{\sum_i (max[X_0 - X_{+i}, X_0 - X_{-i}, 0])^2}$$

CT14 asymmetric PDF errors

2. The MC generation produces N_{rep} asymmetric replicas

$$X^{(k)} = X(\{0\}) + \delta X^{(k)} - \langle \delta X \rangle$$

$$\delta X^{(k)} \equiv \sum_{i=1}^{D} \frac{X_{+i} - X_{-i}}{2} R_i^{(k)} + \frac{1}{2} \sum_{i,j=1}^{D} (X_{+i} + X_{-i} - 2X_0)(R_i{}^{(k)})^2$$

With this definition, $\langle X \rangle = X(\{0\})$: does not fluctuate about $X(\{0\})$

The MC errors can be estimated by **asymmetric** standard deviations,

$$\delta_{68}^{MC,>} X = \sqrt{\langle (X - \langle X \rangle)^2 \rangle_{X > \langle X \rangle}}$$

$$\delta_{68}^{MC,<} X = \sqrt{\langle (X - \langle X \rangle)^2 \rangle_{X < \langle X \rangle}}$$

Alternatively, $\delta_{68}^{MC,\gtrless} X$ can be estimated by 68% central probability intervals for ordered X_i values
(more cumbersome and noisy than the std. deviations)

Comparison with Watt-Thorne algorithm

CTEQ

CT14 algorithm:

$$X^{(k)} = X(\{0\}) + \sum_{i=1}^{D} \frac{X_{+i} - X_{-i}}{2} R_i^{(k)} + \frac{1}{2} \sum_{i,j=1}^{D} (X_{+i} + X_{-i} - 2X_0)(R_i^{(k)})^2 - \langle \delta X \rangle$$

$$\delta_{68}^{MC,\lessgtr} X = \sqrt{\langle (X - \langle X \rangle)^2 \rangle_{X \gtrless \langle X \rangle}}$$

Recommended

Asymmetric algorithm in Watt, Thorne (arXiv:1205.4024)

$$X^{(k)} = X(\{0\}) + \sum_{i=1}^{D} \frac{\partial X}{\partial R_i} R_i^{(k)}$$

$$\frac{\partial X}{\partial R_i} = \begin{cases} X_{+i} - X_0, & R_i^{(k)} > 0 \\ X_0 - X_{-i}, & R_i^{(k)} < 0 \end{cases}$$

Different from the CT14 algorithm if $R_i^{(k)} \neq 0, \pm 1$

We find that separate averaging of positive and negative displacements is essential for recovering the asymmetry of $\delta^{H,\lessgtr} X$ in CT14

Asymmetric standard deviations for PDFs $(X = f)$ ...

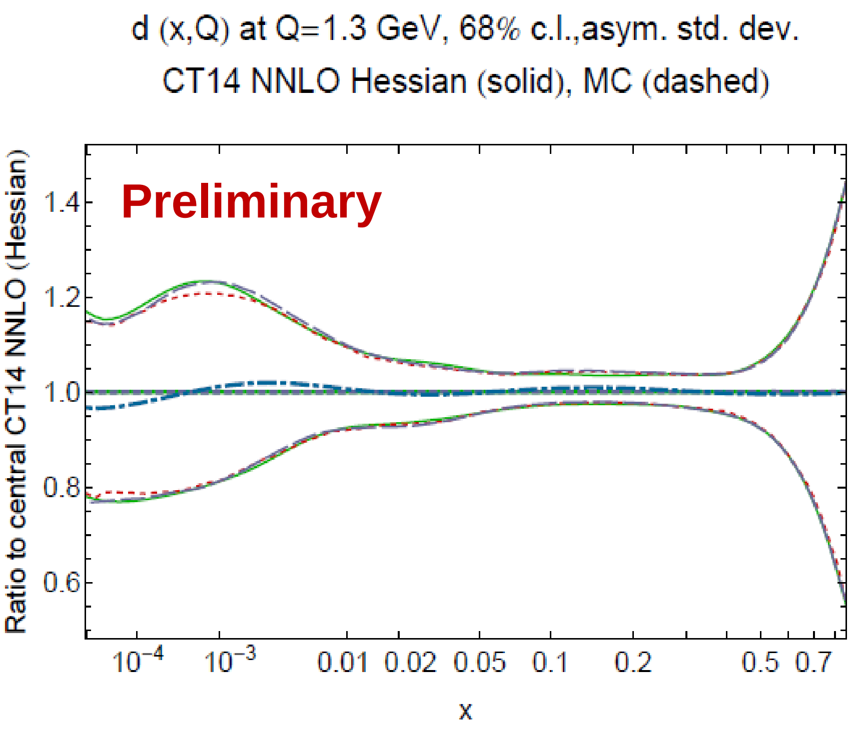

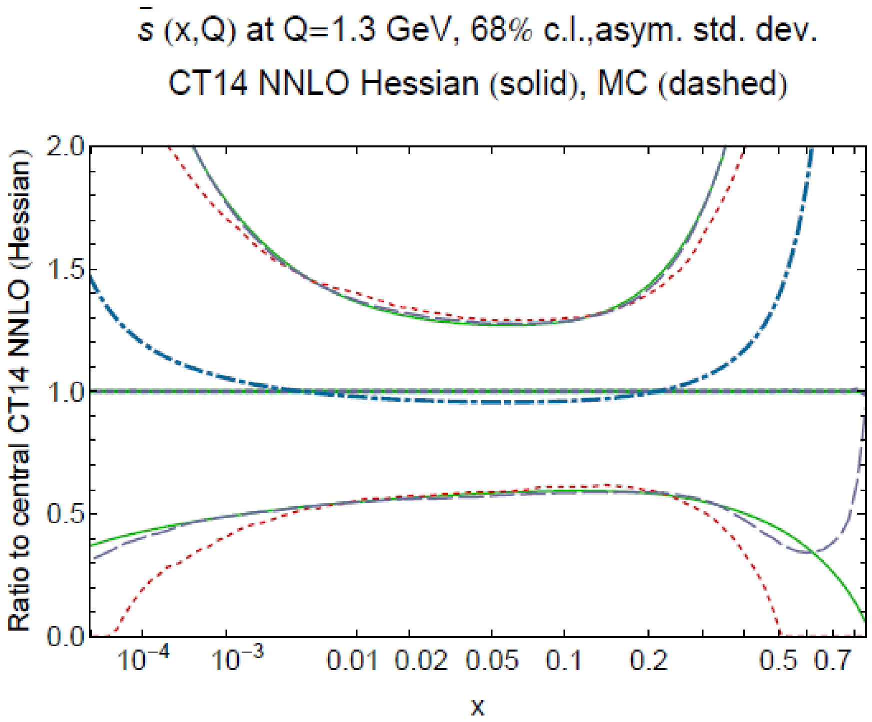

Green: Hessian std. deviation
Red: Symmetric MC std. dev.
Thin blue: Asymmetric MC std. dev.
Thick blue: Asymmetric MC median

Good agreement between green and light blue, smooth behavior

Asymmetric central probability intervals

d (x,Q) at Q=1.3 GeV, 68 and 95% c.l.,asymmetric
CT14 NNLO Hessian (solid), MC (dashed)

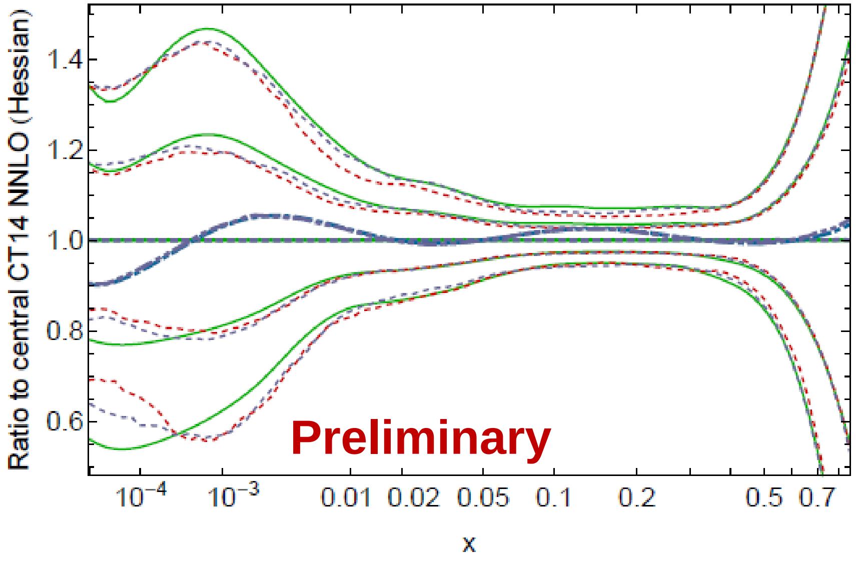

$\bar{s}$ (x,Q) at Q=1.3 GeV, 68 and 95% c.l.,asymmetric
CT14 NNLO Hessian (solid), MC (dashed)

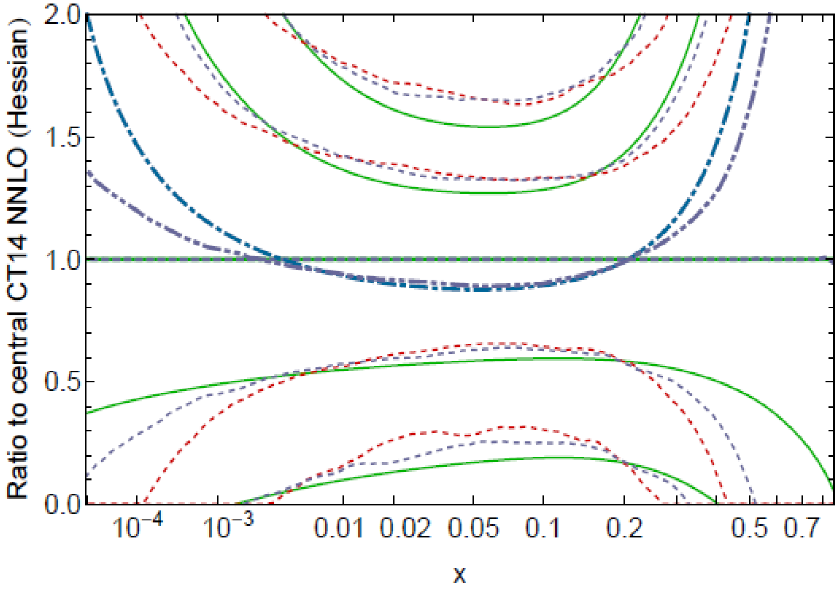

Green: Hessian probability intervals
Red: Symmetric MC generation
Thin blue: Asymmetric MC generation, Watt-Thorne formula
Thick blue: Asymmetric MC median

Probability intervals are more sensitive to behavior of individual replica

Large chi^2 in replicas

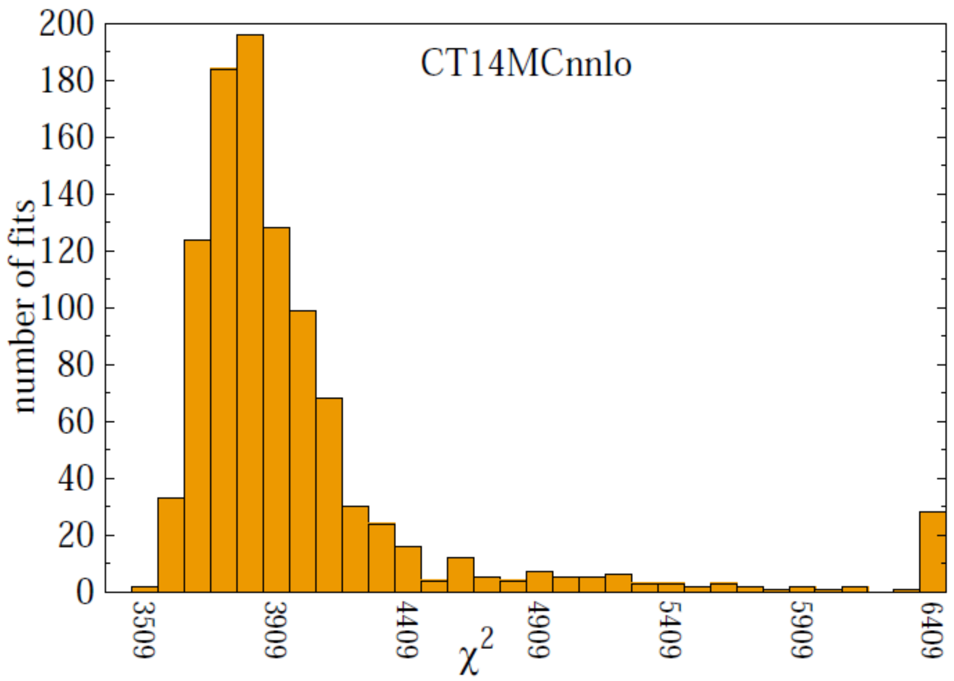

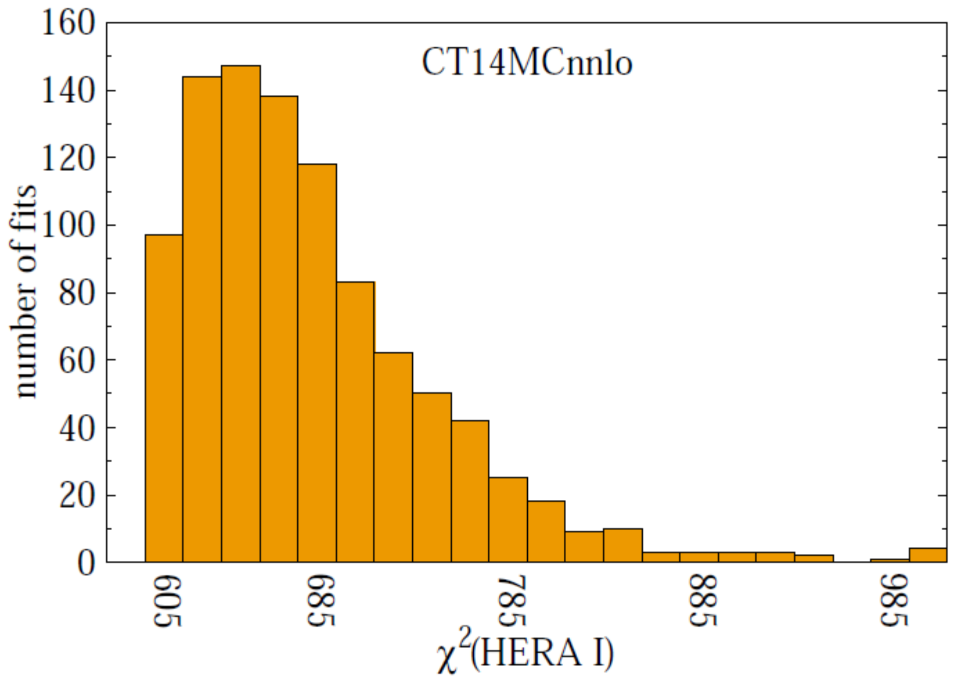

Typical CT14MC replicas sets have large chi^2.
Here, we show chi^2 distributions for 1000 replicas, with about 3000 data points (579 for HERA-I) included in the CT14 fit.

Implications of CMS W^+W^- data to photon PDFs

CT14QED

CMS A A -> W+ W- Data

CERN-PH-EP/2013-084
2013/08/22

CMS-FSQ-12-010

Study of exclusive two-photon production of W^+W^- in pp collisions at $\sqrt{s} = 7$ TeV and constraints on anomalous quartic gauge couplings

The CMS Collaboration*

CT14QED PDFs

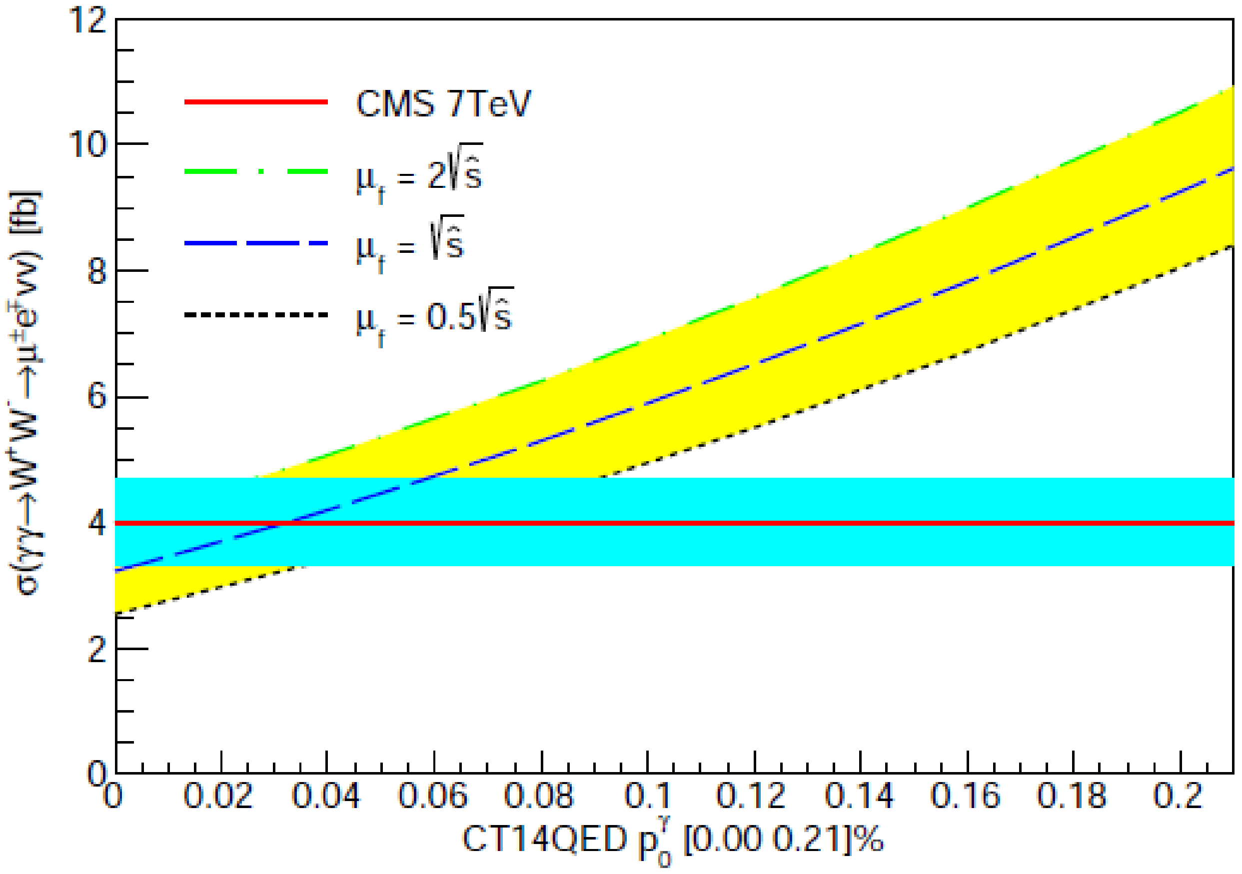

FIG. 1: CT14QED prediction with different scale choices with initial photon momentum fraction varing from 0.00% to 0.21% and the CMS result with uncertainty.

Compare CMS Data to various photon PDFs

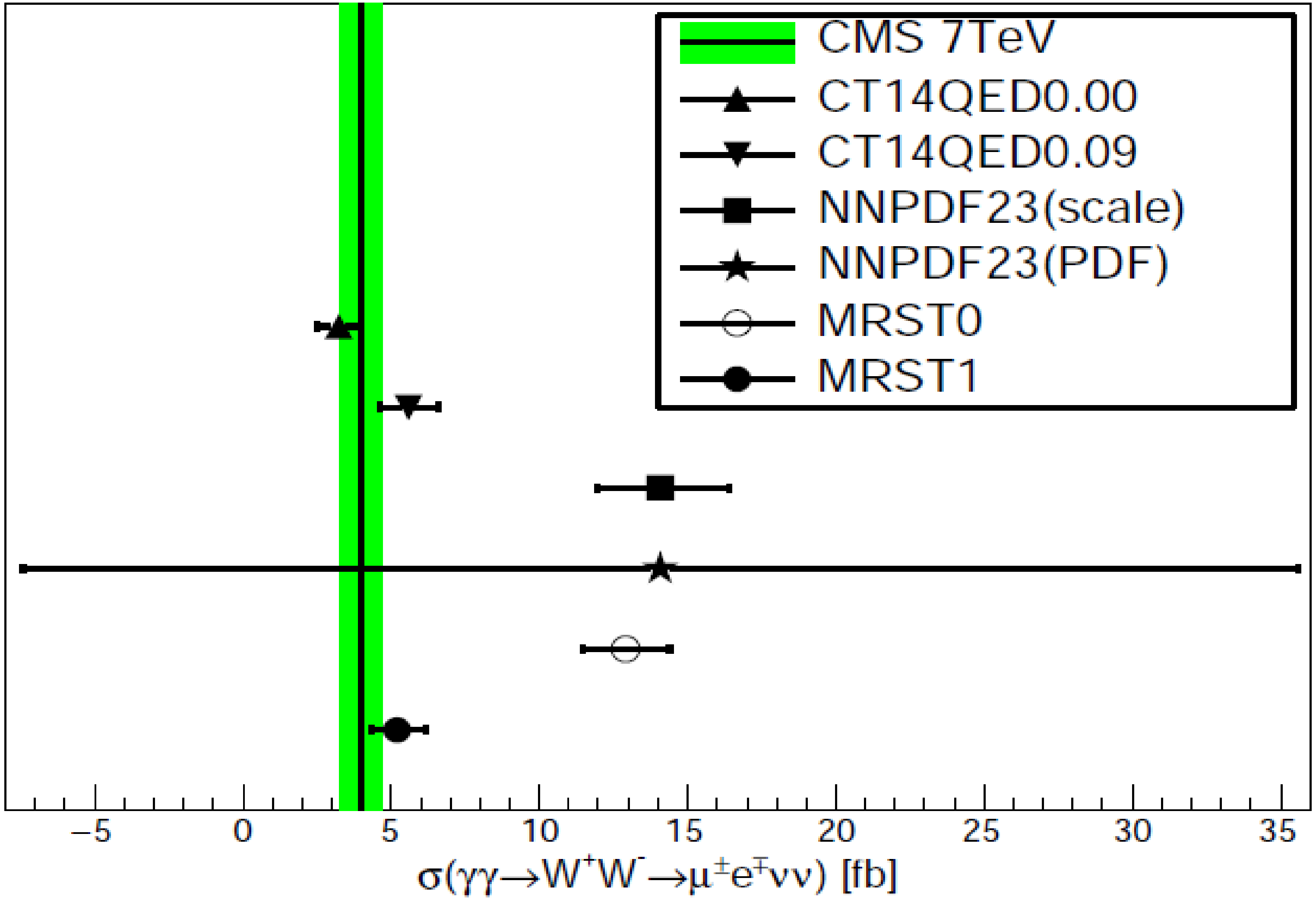

Photon-Photon Luminosity

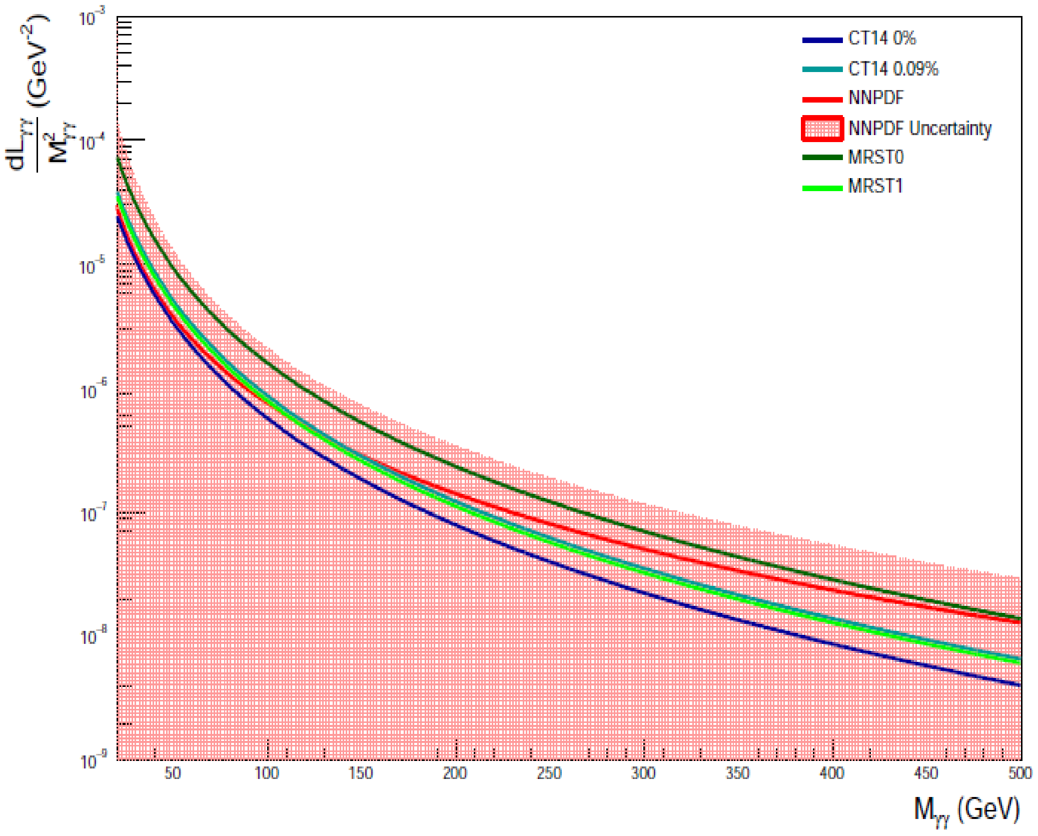

FIG. 4: Photon-photon luminosity for an invariant mass of 20 GeV to 500 GeV for 13 TeV collider energy

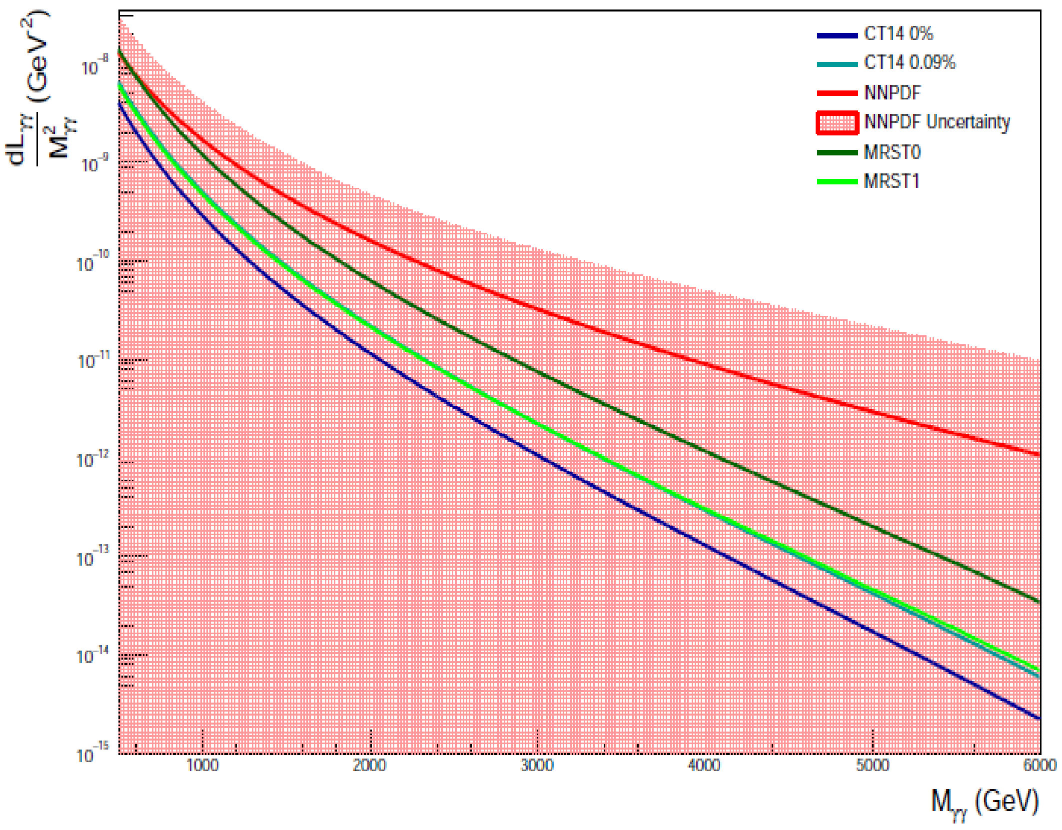

FIG. 5: Photon-photon luminosity for and invariant mass of 500 GeV to 6000 GeV for 13 TeV collider energy

Various photon PDFs at Q=3.2 GeV

C T E Q

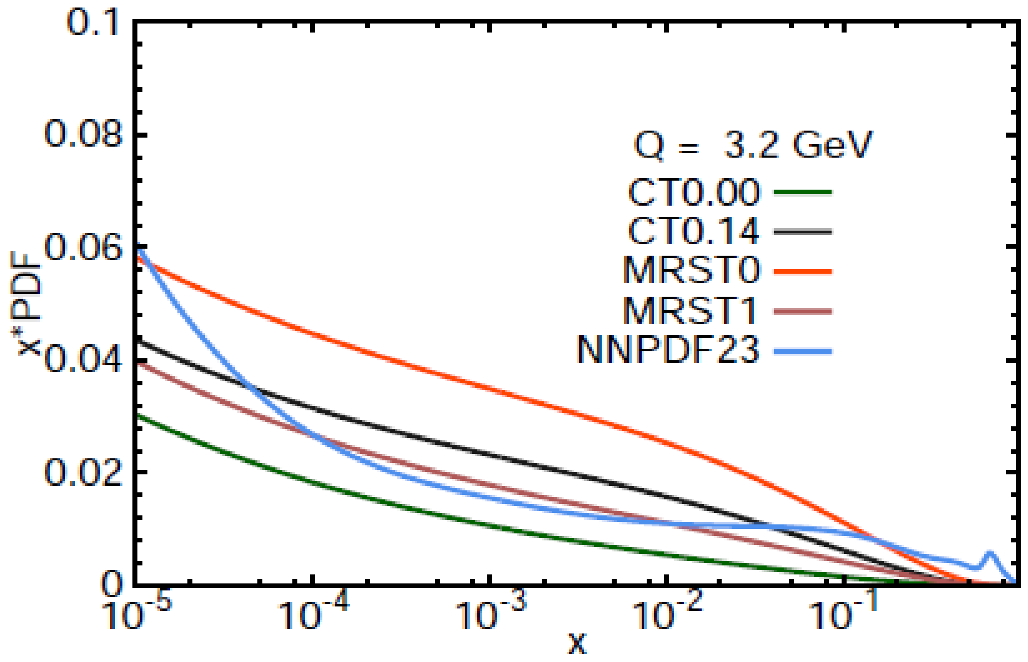

FIG. 10: Comparison of various NLO photon PDFs at the scale $Q = 3.2$ GeV: CT14QED with $p_0^\gamma = 0\%$ (green), CT14QED with $p_0^\gamma = 0.14\%$ (black), MRST2004QED0 using current quark masses (orange), MRST2004QED1 using constituent quark masses (brown), and NNPDF2.3QED with $\alpha_s = 0.118$ and average photon (blue).

Various photon PDFs at Q=85 GeV and 1 TeV

C T E Q

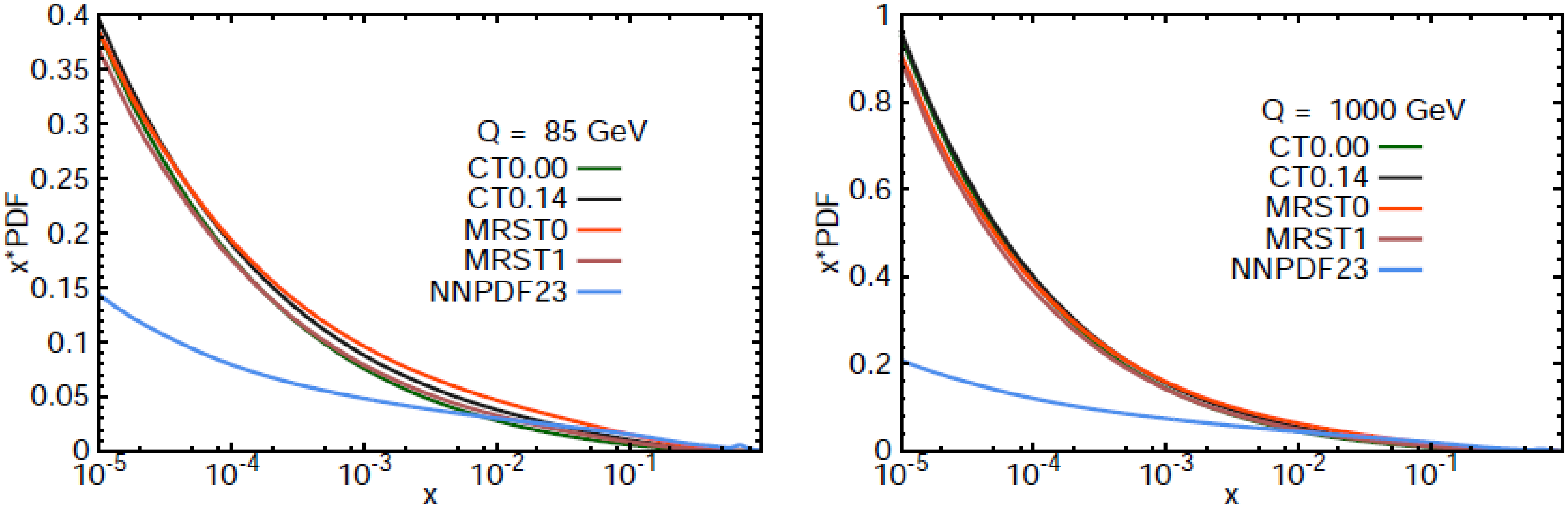

FIG. 11: Comparison of various NLO photon PDFs at the scales $Q = 85$ GeV (left) and $Q = 1$ TeV (right): CT14QED with $p_0^\gamma = 0\%$ (green), CT14QED with $p_0^\gamma = 0.14\%$ (black), MRST2004QED0 using current quark masses (orange), MRST2004QED1 using constituent quark masses (brown), and NNPDF2.3QED with $\alpha_s = 0.118$ and average photon (blue).

Conclusion

- Impact of HERA I + II data on CT PDF analysis: **CT14HERA2**
- Replicas of CT14 PDFs: **CT14MC**
- Implications of CMS W^+W^- data to photon PDFs: **CT14QED**
- We are including more LHC data into the global analysis.

Backup Slides

Photon PDFs

1) Previous studies
   a) MRST   Martin et al., EPJC 39 (2005) 155
      - Radiation off "primordial current quark" distributions
   b) NNPDF   Ball et al., Nuc. Phys. B 877 (2013) 290
      - parametrized fit, predominantly constrained by W, Z, γ^* Drell-Yan
   c) Sadykov   arXiv:1401.1133
      - photon evolution in QCDNum

2) Photon evolution at LO in α and NLO in α_S currently implemented in CTEQ-TEA global analysis package
   a) Alternative parametrization approach
   b) Constrain with DIS + photon data

Photon PDF Parametrization

"Radiative ansatz" for initial Photon PDFs (generalization of MRST choice)

$$\gamma^p = \frac{\alpha}{2\pi}\left(A_u e_u^2 \tilde{P}_{\gamma q} \circ u^0 + A_d e_d^2 \tilde{P}_{\gamma q} \circ d^0\right)$$

$$\gamma^n = \frac{\alpha}{2\pi}\left(A_u e_u^2 \tilde{P}_{\gamma q} \circ d^0 + A_d e_d^2 \tilde{P}_{\gamma q} \circ u^0\right)$$

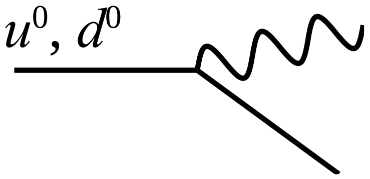

where u^0 and d^0 are "primordial" valence-type distributions of the proton.
Assumed approximate isospin symmetry for neutron.
Here, we take A_u and A_d as unknown fit parameters.

MRST choice: $A_q = \ln\left(Q_0^2 / m_q^2\right)$ "Radiation from **C**urrent **M**ass" – **CM**

We use $u^0 = u^p \circ u^p(x, Q_0)$, $d^0 = d^p \circ d^p(x, Q_0)$
and reduce the number of parameters further (for initial study) by setting

$$A_u = A_d = A_0$$

Now everything effectively specified by one unknown parameter:

$$A_0 \Leftrightarrow p_0^\gamma \equiv p^{\gamma/P}(Q_0)$$ (Initial Photon momentum fraction)

Photon PDFs (in proton)

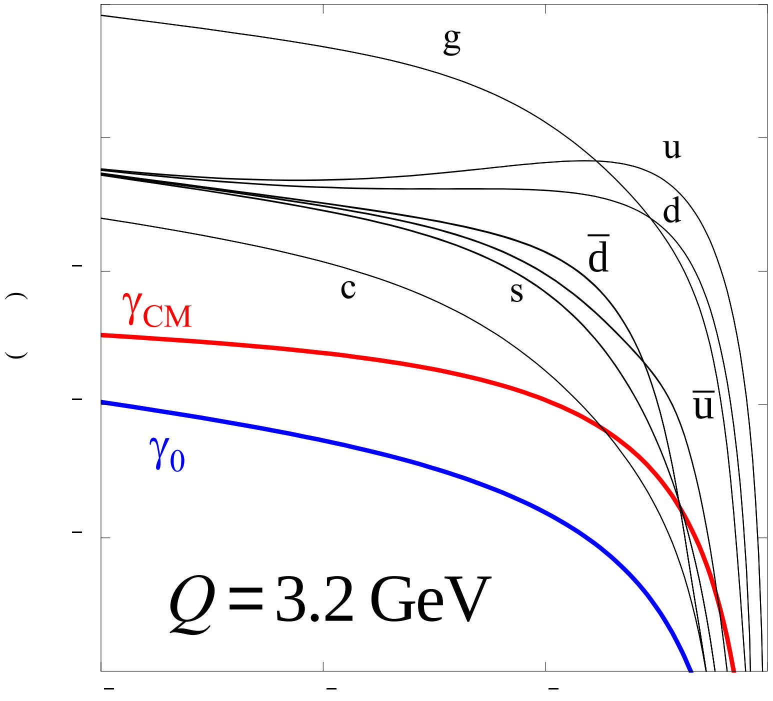

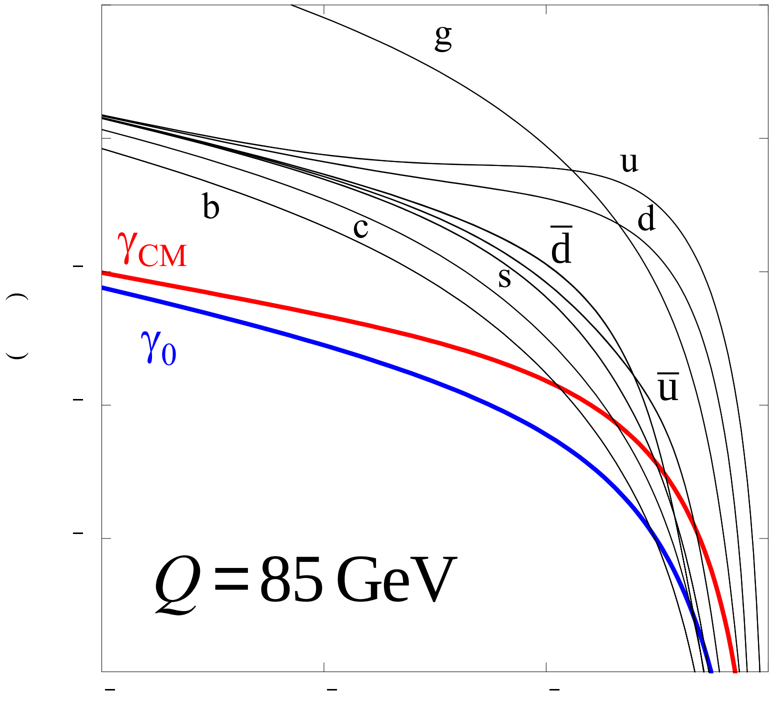

γ momentum fraction:

$p^g(Q)$	$g(x,Q_0)=0$	$g(x,Q_0)_{CM}$
Q = 3.2 GeV	0.05%	0.34%
Q = 85 GeV	0.22%	0.51%

Photon PDF can be larger than sea quarks at large x!

Initial Photon PDF still ← significant at large Q.

Constraining Photon PDFs

1) Global fitting
   - Isospin violation, momentum sum rule lead to constraints in fit
   - We find p_0^g can be as large as ~ 5% at 90%CL, much more than **CM** choice

2) Direct photon PDF probe
   - DIS with observed photon, $ep \to e\gamma + X$
   - Photon-initiated subprocess contributes at LO, and no larger background with which to compete
   - But must include quark-initiated contributions consistently
   - Treat as NLO in α, but discard small corrections, suppressed by $\alpha\,\gamma(x)$.

$ep \to e\gamma + X$

Subprocess contributions:

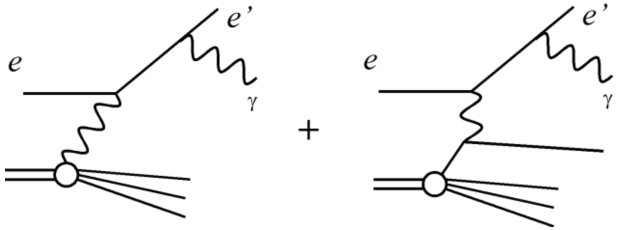

LL Emission off Lepton line

Both quark-initiated and photon-initiated contributions are $\sim \alpha^3$ if $\gamma(x) \sim \alpha$

Collinear divergence cancels (in d=4-2ε) by treating as NLO in α with $\gamma^{\text{bare}}(x) = \gamma(x) + \frac{(4\pi)^\epsilon}{\epsilon}\Gamma(1+\epsilon)\frac{\alpha}{2\pi}\left(P_{\gamma q} \circ q\right)(x)$ (MSbar)

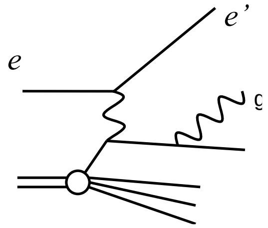

QQ Emission off Quark line

Has final-state quark-photon collinear singularity

QL Interference term

Negligible < about 1% (but still included)

Previous calculations:

quark-initiated only – (GGP) Gehrmann-De Ridder, Gehrmann, Poulson, PRL 96, 132002 (2006)

photon initiated only – (MRST), Martin, Roberts, Stirling, Thorne, Eur. Phys. J. C 39, 155 (2005)

Limits on Photon PDF

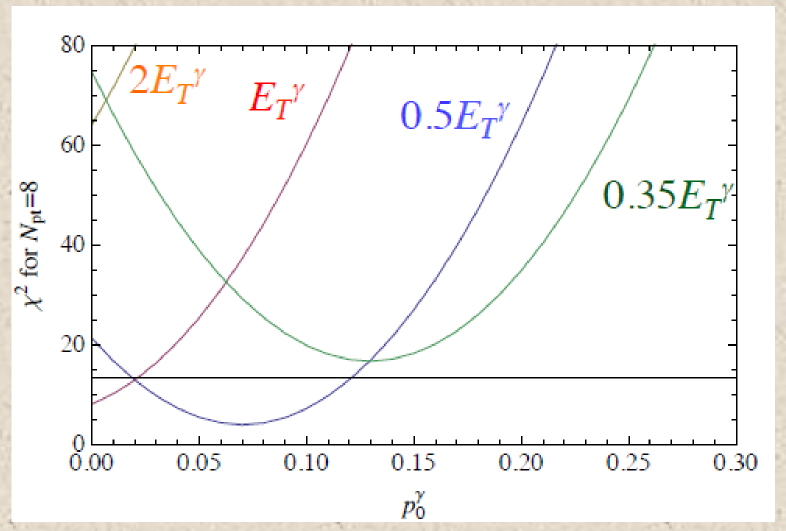

Smooth Isolation

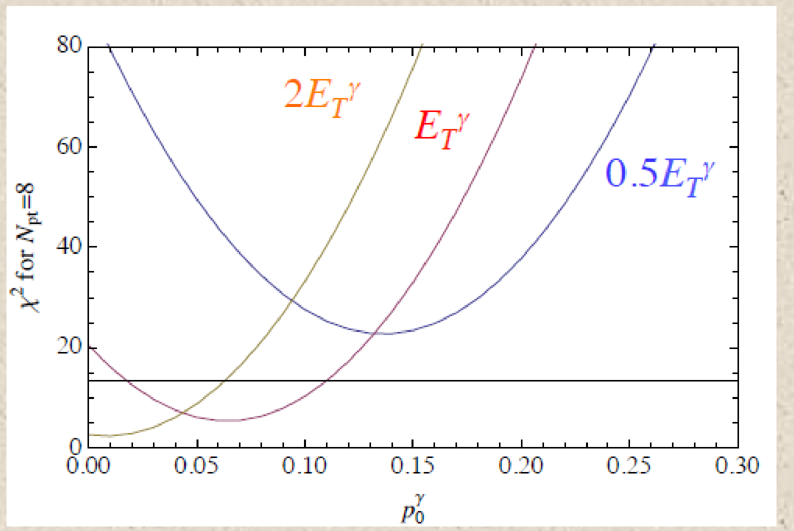

Sharp Isolation

•Different χ^2 curves for choice of isolation and scale μ_F
•90% C.L. for N_{pt} = 8 corresponds to $\chi^2 = 13.36$

•Obtain p_0^g £ 0.14% at 90 % C.L. independent of isolation prescription

(More generally, constrains $\gamma(x)$ for $10^{-3} < x < 2x10^{-2}$.)

•"Current Mass" ansatz has $\chi^2 > 45$ for any choice of isolation and scale